CDF/ANAL/TOP/CDFR/10201
Draft 1.2
July 15, 2010

Measuring the $t\bar{t}$ background to the Higgs search in the MET+jets channel

D. Bortoletto, Q. Liu, F. Margaroli, K. Potamianos
Purdue University

Abstract

We report on the first measurement of the production cross section of top quark pairs in events with large missing transverse energy, two or three high-P_T jets, where at least one is identified as a b-jet by using SECVTX and/or JETPROB b-tagging algorithms. A veto on loosely identified electrons and muons is applied. We reduce the dominant QCD multijet background using neural networks, and then use another neural network to isolate the $t\bar{t}$ signal from the remaining backgrounds. Analyzing $5.7\,\mathrm{fb}^{-1}$ of data, we expect to measure the $t\bar{t}$ cross section with a 7% statistical uncertainty, and a 15% overall uncertainty. The measured cross section amounts to $\sigma_{t\bar{t}} = 7.12^{+1.20}_{-1.12}\,(stat. + syst.)\,pb$.

Contents

1 Introduction **3**

2 Signal and Backgrounds **4**
2.1 Signal modeling 4
2.2 Background modeling 4
2.2.1 QCD Multijet: a data-driven model 4
2.2.2 Monte Carlos 5

3 Event Selections **6**
3.1 Preselection 6
3.2 Neural network based event selection 7
3.3 Analysis Regions 12

4 $t\bar{t}$ Cross-section Measurement **15**
4.1 Discriminating the signal from remaining backgrounds 15
4.2 Systematics 18
4.3 Likelihood Fit 21
4.4 Results 23

DRAFT JULY 15, 2010

5 Summary **24**

A Lepton Identification **26**

B Tag Rate Matrix **27**

C Validation Plots **28**

C.1 TRM 29
C.2 QCDCR 34
C.3 EwkCR 39
C.4 PreSelection 44
C.5 Lower_ttbar 49
C.6 Inter_ttbar 54
C.7 SigReg_ttbar 59

DRAFT JULY 15, 2010

1 Introduction

The measurement of the top quark properties allows one to verify the consistency of the standard model. At the Fermilab Tevatron Collider top quarks are produced mostly in pairs and the measurement of the $t\bar{t}$ cross section tests the next-to-leading-order (NLO) QCD calculations.

The top quark has been discovered in semileptonic decays thanks to the good S/B ratio and large acceptance. Since then, the all-hadronic and dileptonic decays have been used for measuring this quantity. The $t\bar{t}$ production cross section has also been measured in the MET+$\geq$ 4 jets signature [1, 2]. That signature collects semileptonic top decays where one lepton is not identified, thus having large acceptance to tau decays.

We are interested in the MET+2/3 jets, and no leptons signature. In fact, due to the limited lepton identification capabilities at the CDF, a large fraction of dileptonic or lepton+jets top pair production don't pass the lepton selection criteria. The measurement of the $t\bar{t}$ cross section in this sample would thus complete the study of all possible decays of top pairs. This measurement is complementary to existing measurement and can be combined with those to achieve greater precision and test more stringently QCD NLO predictions.

The top quark pair production cross section is just a fraction of the background events to the SM Higgs search in the MET+b-jets channel [3] but still it is much larger than the SM Higgs signal itself. The single top quark cross section measurement has been measured in this sample [4, 5] but with low precision. The observation of $t\bar{t}$ production cross section in this sample would thus provide a much stronger test of the background model and of the tools used in the search for the Higgs boson in this sample.

To improve the signal-to-background ratio (s/b), we select jets identified as originating from b quarks using b-tagging algorithms. Even after these requirements, the s/b is still too low to achieve sensitivity to top quark pair production. We further exploit the kinematic and topological characteristics of $t\bar{t}$ events using neural networks to isolate the signal from the dominant QCD background and subsequently from the remaining backgrounds.

DRAFT JULY 15, 2010

2 Signal and Backgrounds

2.1 Signal modeling

We use in this analysis simulated $t\bar{t}$ events generated with Pythia 6.2 assuming a top quark mass of $172.5\,\mathrm{GeV}/c^2$, i.e. the nominal tt1s25 sample.

2.2 Background modeling

2.2.1 QCD Multijet: a data-driven model

The most significant background of the analysis is the QCD multijet production. Although these processes generally do not produce neutrinos, mismeasured jet energies do result in imbalance in the measured transverse energy by which the QCD events can pass the basic selection. Furthermore, QCD b quark pair production yields neutrinos whenever one b-hadron decays semi-leptonically, thus giving additional $\not\!\!E_T$. The background sources for this final state are due mainly to QCD production of heavy-quark pairs ($b\bar{b}$ and $c\bar{c}$) and jets falsely tagged as b-jets.

Because of the high production rate for QCD at a hadron collider and the large statistics needed in order to describe this process adequately in an analysis looking for a small signal, the Monte Carlo simulation of an acceptable amount of QCD events is prohibitive. Moreover, the systematic uncertainties associated with the Monte Carlo simulation of QCD jet production are high. For these reasons, we estimate the QCD background solely from data using Tag Rate Matrix(Appendix B). The details of this estimation can be found here [12]. A summary is given below.

Events collected by the $\not\!\!E_T$+jets trigger are expected to be composed mostly of QCD production of light flavor jets. We model the heavy flavor jets QCD rate and distributions by weighting events without any b-tagging requirement by the probability to tag a jet as a b-jet. This probability is extracted from events depleted in $t\bar{t}$ signal, *i.e.* events with $50 \leq \not\!\!E_T \leq 70$ GeV and $\Delta\phi(\vec{\not\!\!E}_T, \vec{j_2}) < 0.4$, and two or three jets. The tag rate per jet is evaluated as a ratio of $b-$tagged to fiducial jets, where the fiducial jets are the ones in the kinematic region where the secondary vertex detection efficiency is nonzero. The tag rate is parametrized in terms of variables sensitive to both the efficiency of the identification of true heavy-flavored objects and the rate of false tags. These variables are the jet E_T, the absolute value of the jet η, the scalar sum of the transverse energies of the jets in the event (H_T), and the fraction of jet p_T carried by the charged particles inside the jet which are significantly displaced from the collision point. To compute the last quantity, all charged particles satisfying $0.5 \leq p_T \leq 200$ GeV/c are used, and they are required to have the distance of closest approach to the beamline (d_0) significantly displaced from the beamline, *i.e.* $|d_0/\sigma_{d_0}| > 2.5$ where σ_{d_0} is the uncertainty on d_0.

The tag rate parametrization is then used to estimate the probability that a fiducial jet in the signal candidate sample is tagged. We construct three independent

DRAFT July 15, 2010

parametrizations to estimate the background in events with exactly one SecVTX-tagged jet (1S), two SecVTX-tagged jets (2S category), and one SecVTX-tagged and one JetProb-tagged jet (SJ category). Events which belong to both 2S and SJ categories are assigned to the 2S subsample. Events with three b-tagged jets are discarded. In this way the three selections are orthogonal by construction so that an event can belong to only one category.

By summing the probability of b-tagging each fiducial jet in each b-tag subsample and weighting the rate and distributions of data events before any $b-$tagging requirement (pretag sample), we predict the rate of QCD b-tagged jet multijet production background events and its kinematic distributions.With respect to our previous analysis, we predict the kinematic properties of events with any number and combination of tagged jet QCD background from the pretag sample. The parametrizations do not completely account for the fact that events with pair production of heavy flavor have enhanced probability to be tagged. For this reason, the normalization of the background events arising from the simple application of the parametrization needs to be scaled.

2.2.2 Monte Carlos

The other backgrounds to top quark pair production in this signature come from the production of a W or a Z boson in association with jets. We normalized the W and Z boson + heavy flavor jets backgrounds using a factor of 1.3 with respect to the LO predictions.

For the simulated diboson samples we use LO cross sections scaled by a factor corresponding to the ratio between the NLO and LO cross section prediction in MCFM [9]. The boson decays are set to be inclusive. An 11.5% uncertainty on the MCFM cross section is assigned to the diboson normalization [10].

Table 1: Physics processes considered, how we model them, how we normalize them and why

Process	Modeling	Cross Sections	Source
$t\bar{t}$	Pythia	to be measured	
QCD/mistags	data-driven estimation	-	QCD control regions
W+jets/Z+jets	ALPGEN + Pythia	1.3× LO cross sec	
single top (s-chan)	MadGrapgh	1.05± 0.17pb	[7, 8]
single top (t-chan)	MadGrapgh	2.12± 0.32pb	
WW	Pythia	12.4 ± 1.4	MCFM [9]
WZ	Pythia	3.7 ± 0.4	MCFM [9]
ZZ	Pythia	3.6 ± 0.4	MCFM [9]

DRAFT JULY 15, 2010

3 Event Selections

Since we are looking at events with non-identified electrons and muons, or hadronically decaying taus, we use a trigger devised to select events on the presence of two calorimetric jets and large missing transverse energy. The analysis region can be summarized as:

- $\not\!\!E_T > 50$ GeV, $E_T^{j1} > 35$ GeV, $E_T^{j2} > 25$ GeV and $E_T^{j3} > 15$ GeV
- 2 or 3 jets, with $\eta < 2$ and j_1 or j_2 central ($\eta < 0.9$), $\Delta R(j_1, j_2) > 1$
- Unidentified leptons (reversing loose lepton ID cuts). See the lepton ID in Appendix A.
- One or both of the two leading jets are b-tagged. We also divide them into three exclusive tagging categories:
  - 1S: One of the two leading jets is SecVTX tight tagged, the other is not tagged.
  - SS: Both leading jets are tight tagged by SecVTX.
  - SJ: One of the two leading jets is SecVTX tight tagged and the other is tagged by JetProb.

3.1 Preselection

The $\not\!\!E_T$ plus jets trigger efficiency is computed using data collected with a high p_T muon, and with data collected with a trigger requiring the presence of a jet with $E_T > 20\,\text{GeV}$ [13]. Trigger efficiencies are calculated for all three levels of the CDF trigger, and are then parametrized as a function of $\not\!\!E_T$ and E_T of the jets. The systematic uncertainties originating from the choice of the samples used in the efficiency calculations are large at small $\not\!\!E_T$, and therefore we require every event to have $\not\!\!E_T > 50\,\text{GeV}$. The trigger is nearly 100% efficient if the jets with the highest and second highest transverse energies satisfy the conditions $E_T^{j_1} > 35\,\text{GeV}$ and $E_T^{j_2} > 25\,\text{GeV}$ respectively. Additionally, we require the spatial separation between the two leading E_T jets to be greater than $\Delta R = 1$, where $\Delta R = \sqrt{\Delta\eta^2 + \Delta\phi^2}$ is the distance in the $\eta - \phi$ space between the two jet centroids, in order to avoid jet merging performed by the level 2 jet clustering algorithm. A small fraction of events do not pass the level 1 requirements due to a hardware problem, and are recovered with a trigger on inclusive jets [14].

At this stage of the analysis, the vast majority of the background events are QCD events where mismeasurement of the jet energies gives the very large $\not\!\!E_T$. These events are characterized by having $\vec{\not\!\!E}_T$ aligned in the axymuthal angle ϕ with one of the jets ($\vec{j_i}$) in the event, where the index i runs over the jets in the event. We require $\Delta\phi(\vec{\not\!\!E}_T, \vec{j_1}) > 1.5$ and $\Delta\phi(\vec{\not\!\!E}_T, \vec{j_{2,3}}) > 0.4$ to reject such events. These cuts remove about an order of magnitude of QCD events, but still leave us with a poor s/b, where

DRAFT JULY 15, 2010

the majority of the background is still composed of QCD multijet production. Finally, we require the presence of at least one jet identified as originating from a b quark. We divide the sample in the three exclusive subsamples 1S, SJ and 2S. This requirement brings the s/b ratio over the three subsamples to 1/20 for 1S, 1/7 for SJ, 1/3 for SS. The mulijet background is still the dominant background in all three subsamples. Thus we need to exploit additional properties of these events in order to further increase the purity of the sample.

3.2 Neural network based event selection

We introduce here a neural network approach to the event selection to recognize and separate QCD multijet events with mismeasured jets in which $\not\!\!E_T$ is due to instrumental effects from events with $\not\!\!E_T$ originating from neutrinos. In addition, the neural network is designed to reject events with mis-tagged light flavor jets. Using a neural network instead of a "cut-cascade" approach to event selection allows the exploitation of the correlation between the many observables which provide discrimination between signal and backgrounds, and gives a single output thus simplifying the determination of the optimal cut.

A neural network based event selection to suppress the overwheling QCD background has been used for the first time in the $t\bar{t}$ all-hadronic cross section measurement to greatly increase sensitivity [15, 16].

The neural network model chosen is the Multi Layer Perceptron as implemented in the TMVA package, found in ROOT.

In this analysis the charged particle spectrometer is used in an innovative way to discriminate between events containing high energy neutrinos and QCD events. This studies are documented here [6]. We introduce here the imbalance in the momentum flow in the transverse plane, and name it missing transverse momentum, or $\vec{\not\!\!p}_T$, in analogy with the missing transverse energy, $\vec{\not\!\!E}_T$. To compute $\vec{\not\!\!p}_T$, we select charged particles with $0.5 < p_T < 200\,\mathrm{GeV}/c$ and z position at the beamline compatible with the z position of the primary vertex. The missing transverse momentum is then defined as $\vec{\not\!\!p}_T = -\sum_{tracks} \vec{p_T}$. In collisions producing high energy neutrinos, the magnitude of $\vec{\not\!\!p}_T$ ($\not\!\!p_T$) is proportional to the neutrino energy, while $\vec{\not\!\!p}_T$ provides a good estimate of the neutrino direction. In QCD events with the $\not\!\!E_T$ plus jets topology, where high energy neutrinos are rarely produced and the fluctuation of the charged-to-neutral ratio in jet fragmentation is the primary source of imbalance of the total transverse momentum, the magnitude of $\not\!\!p_T$ is expected to be relatively low, and the vector $\vec{\not\!\!p}_T$ to be often aligned in direction with the momentum of one of the most energetic jets.

As inputs into our neural network we use the following variables which describe the energy and momentum flow in the detector: the absolute amount of the missing transverse energy, $\not\!\!E_T$; the absolute amount of the missing transverse momentum $\not\!\!p_T$; the $\not\!\!E_T$ significance defined as $\not\!\!E_T/\sqrt{\sum E_T}$, where $\sum E_T$ is a scalar sum over the energy deposited in the calorimeter towers; the ratio of $\not\!\!E_T$ to H_T; the ratio of $\not\!\!H_T = |-\sum_{jets} \vec{p_T}|$

DRAFT JULY 15, 2010

and $\not{E}_T$; the invariant mass of $\vec{\not{E}}_T$, $\vec{j_1}$ and $\vec{j_2}$, $M(\vec{\not{E}}_T, \vec{j_1}, \vec{j_2})$.

We use the following angular variables: the azimuthal difference between $\vec{\not{p}}_T$ and $\vec{\not{E}}_T$, $\Delta\phi(\vec{\not{p}}_T, \vec{\not{E}}_T)$; the maximum of $\Delta\phi$ between any two jets $\vec{j_i}, \vec{j_k}$, $Max(\Delta\phi(\vec{j_i}, \vec{j_k}))$; the maximum of the difference in R between any two jets $\vec{j_i}, \vec{j_k}$, $Max(\Delta R(\vec{j_i}, \vec{j_k}))$; the minimum of the difference in ϕ between $\vec{\not{E}}_T$ and any jet $\vec{j_i}$, $Min(\Delta\phi(\vec{\not{E}}_T, \vec{j_i}))$; the minimum of the difference in ϕ between the $\vec{\not{p}}_T$ and any jet $\vec{j_i}$, $Min(\Delta\phi(\vec{\not{p}}_T, \vec{j_i}))$; the difference in the azimuthal plane between the axis defined by the two leading jets in their rest frame, and their vector sum in the lab frame, ϕ^*; the event sphericity [11].

We also use variables that discriminate between the fragmentation properties of heavy flavor quark jets and jets originating from light flavor quarks or gluons: by taking the charged particles with $p_T > 0.5\,\mathrm{GeV}/c$ and $|d_0/\sigma_{d_0}| > 2.5$ and contained inside the jet cone, we build the variable $\sum {p_T}^{chgd}/{p_T}^{j}$ for the E_T leading and second leading jets. The 15 variables used as inputs to the neural network are summarized in Table 2. And the shape comparison plots are shown in Figure 1.

Table 2: Input variables to the neural network devised to suppress the multijet background.

Variable	Description
$\not{E}_T$	Absolute amount of the missing transverse energy
$\not{p}_T$	Absolute amount of the missing transverse momentum
$\not{E}_T/\sqrt{\sum E_T}$	Missing E_T significance
$\not{E}_T/H_T$	Ratio of $\not{E}_T$ to H_T
$\not{H}_T$ / $\not{E}_T$	Ratio of $\not{H}_T$ to $\not{E}_T$
$M(\vec{\not{E}}_T, \vec{j_1}, \vec{j_2})$	Invariant mass of $\not{E}_T$, $\vec{j_i}$ and $\vec{j_2}$
$\Delta\phi(\vec{\not{E}}_T, \vec{\not{p}}_T)$	Azymuthal difference between $\not{E}_T$ and $\not{p}_T$
$Max(\Delta\phi(\vec{j_i}, \vec{j_k}))$	Maximum of $\Delta\phi$ between any two jets $\vec{j_i}, \vec{j_k}$
$Max(\Delta R(\vec{j_i}, \vec{j_k}))$	Maximum of ΔR between any two jets $\vec{j_i}, \vec{j_k}$
$Min(\Delta\phi(\vec{\not{E}}_T, \vec{j_i}))$	Minimum of $\Delta\phi$ between $\vec{\not{E}}_T$ and any jet $\vec{j_i}$
$Min(\Delta\phi(\vec{\not{p}}_T, \vec{j_i}))$	Minimum of $\Delta\phi$ between $\vec{\not{p}}_T$ and any jet $\vec{j_i}$
ϕ^*	$\Delta\phi$ of $(\vec{j^1}, \vec{j^2})$ axis in their rest frame, and their vector sum in the lab frame
Sphericity	$S = \frac{3}{2}(\lambda_2 + \lambda_3)$ [11]
$\sum {p_T}^{chgd}/{p_T}^{j_1}$	Fraction of ${p_T}^{j_1}$ carried by charged particles displaced from the primary vertex
$\sum {p_T}^{chgd}/{p_T}^{j_2}$	Fraction of ${p_T}^{j_2}$ carried by charged particles displaced from the primary vertex

The QCD background kinematics do not vary significantly with the heavy flavor content so only one neural network is used for the three b-tagged subsamples. We use the nominal $t\bar{t}$ MC sample for the signal in the training; as for the background, we use the multijet background model described previously. All samples are split into two subsamples: one for training the neural network, and one for making predictions of the

DRAFT, TOBY ISAACS

neural network output and for testing for overtraining. The distributions for training and testing samples are in good agreement. Figure 2 shows the distribution of the value of the output node, $\mathrm{NN_{QCD}}$.

By requiring $\mathrm{NN_{QCD}} >$ -0.5, we reduce the overall background contribution by 65%, while keeping 95% of the signal. This requirement brings the s/b ratio over the three subsamples to 1/7 for 1S, 1/3 for SJ, 1/1.5 for SS, i.e. about a factor of 2 better with negligible signal loss.

The signal significance $s/\sqrt{s+b}$ is increased by 55%, from 6.95 to 10.77.

DRAFT JULY 15, 2010

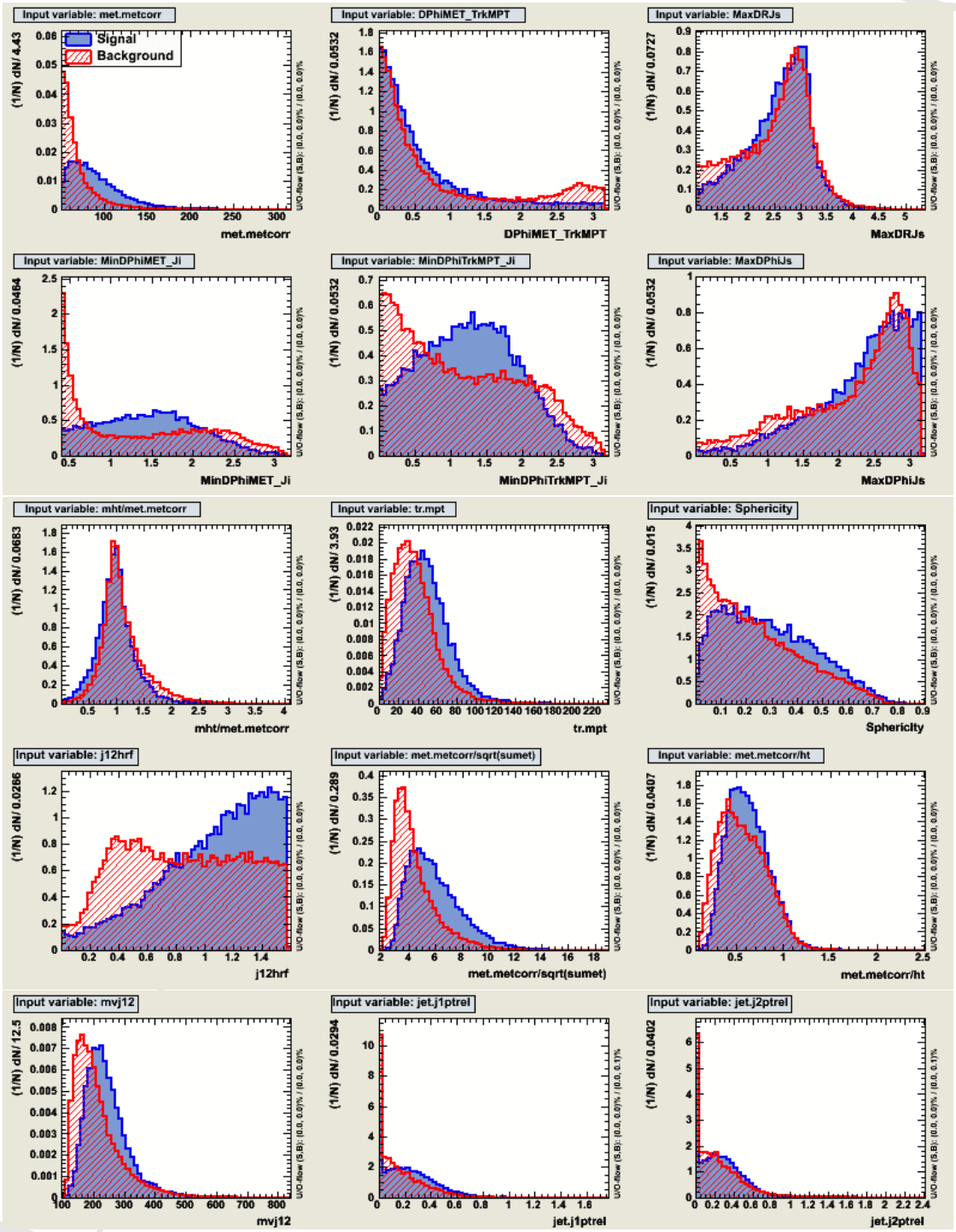

Figure 1: The 15 NN_{QCD} inputs in TMVA

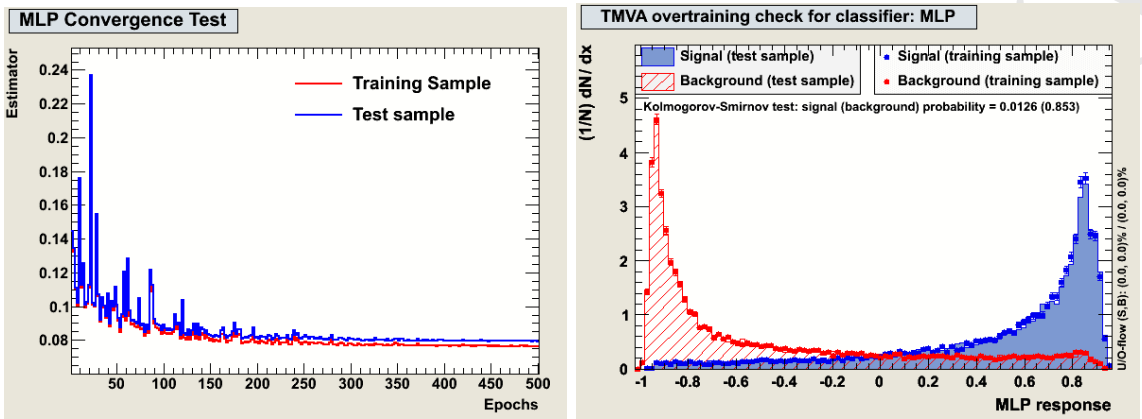

Figure 2: NN_{QCD} output, with overtraining check

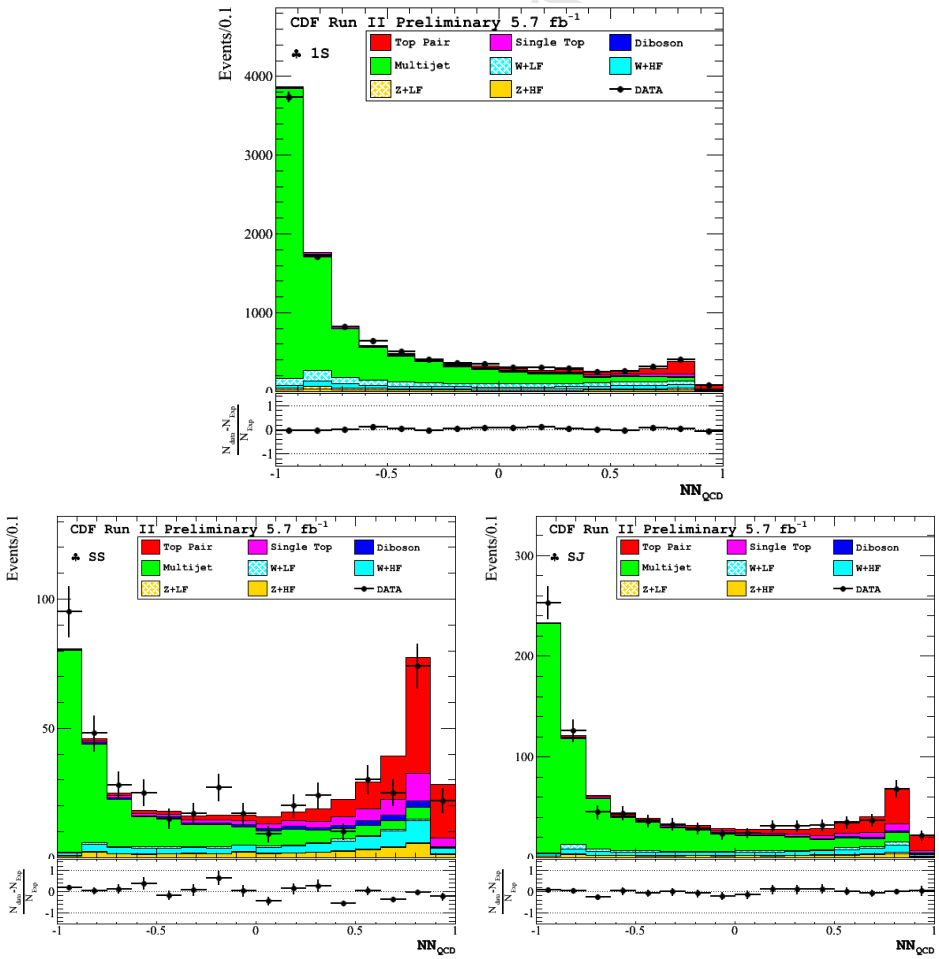

Figure 3: NN_{QCD} distribution in preselection region, where the multijet is normalized to data.

3.3 Analysis Regions

By using the topological cuts and Neural Networks, we define several control regions for validation purpose and also finalize the signal region.

- TRM: a QCD dominant region for multijet model to derive tag-rate-function
  - All leptons are vetoed using the loose lepton ID
  - $\Delta\phi(\vec{\not{E}_T}, \vec{j_2}) < 0.4$ and $50 < \not{E}_T < 70$
- QCDCR: a QCD dominant region to validate multijet model
  - All leptons are vetoed using the loose lepton ID
  - $\Delta\phi(\vec{\not{E}_T}, \vec{j_2}) < 0.4$ and $\not{E}_T > 70$
- EwkCR: a region to validate electroweak Monte Carlo production
  - Minimum 1 loose lepton is required
  - $\Delta\phi(\vec{\not{E}_T}, \vec{j_1}) > 1.5$ and $\Delta\phi(\vec{\not{E}_T}, \vec{j_{2,3}}) > 0.4$
- Lower NN_{QCD} region: a region to validate multijet model and its f_{scale}
  - $\Delta\phi(\vec{\not{E}_T}, \vec{j_1}) > 1.5$, $\Delta\phi(\vec{\not{E}_T}, \vec{j_{2,3}}) > 0.4$ and no lepton, with $NN_{QCD} < -0.8$
- Intermediate NN_{QCD} region: a region to derive multijet model f_{scale} for signal region
  - $\Delta\phi(\vec{\not{E}_T}, \vec{j_1}) > 1.5$, $\Delta\phi(\vec{\not{E}_T}, \vec{j_{2,3}}) > 0.4$ and no lepton, with $-0.8 < NN_{QCD} < -0.5$
- Signal Region: the region with high signal sensitivity to calculate $t\bar{t}$ cross-section
  - $\Delta\phi(\vec{\not{E}_T}, \vec{j_1}) > 1.5$, $\Delta\phi(\vec{\not{E}_T}, \vec{j_{2,3}}) > 0.4$ and no lepton, with $NN_{QCD} > -0.5$

DRAFT JULY 15, 2010

	1S			SS			SJ		
Top Pair	15.1	±	1.0	3.2	±	0.3	3.4	±	0.4
Single Top	5.4	±	0.9	1.2	±	0.2	1.0	±	0.2
Diboson	4.7	±	0.7	0.3	±	0.1	0.4	±	0.1
Multijet	74292.2	±	4457.5	4807.7	±	783.7	9006.3	±	1161.8
W+LF	36.5	±	11.5	0.5	±	0.4	1.6	±	0.7
W+HF	23.8	±	7.3	1.9	±	0.6	2.9	±	1.0
Z+LF	9.6	±	3.0	0.1	±	0.0	0.4	±	0.1
Z+HF	104.6	±	32.5	8.1	±	3.0	12.1	±	4.2
DATA	74492			4823			9028		
Tot. Exp.	74492.0	±	4457.7	4823.0	±	783.7	9028.0	±	1161.8

Table 3: Acceptance table in TRM

	1S			SS			SJ		
Top Pair	18.6	±	1.3	3.8	±	0.4	4.6	±	0.5
Single Top	3.8	±	0.7	0.8	±	0.2	0.9	±	0.2
Diboson	3.3	±	0.5	0.1	±	0.0	0.3	±	0.1
Multijet	17970.8	±	1078.2	1087.3	±	177.2	2657.6	±	342.8
W+LF	41.3	±	13.0	1.0	±	0.5	1.4	±	0.6
W+HF	18.4	±	5.7	1.5	±	0.5	2.4	±	0.8
Z+LF	7.2	±	2.2	0.1	±	0.0	0.4	±	0.2
Z+HF	38.6	±	12.2	4.4	±	1.7	6.4	±	2.4
DATA	18102			1099			2674		
Tot. Exp.	18102.0	±	1078.4	1099.0	±	177.2	2674.0	±	342.8

Table 4: Acceptance table in QCDCR

	1S			SS			SJ		
Top Pair	502.9	±	33.4	151.8	±	15.2	125.4	±	13.4
Single Top	128.6	±	22.2	24.5	±	4.8	19.2	±	3.8
Diboson	53.8	±	7.2	5.5	±	1.0	4.9	±	0.8
Multijet	608.0	±	36.5	5.7	±	0.9	57.2	±	7.4
W+LF	223.1	±	68.7	3.5	±	1.3	7.2	±	2.5
W+HF	306.6	±	94.2	28.8	±	9.7	27.3	±	9.0
Z+LF	32.6	±	10.0	0.4	±	0.2	1.3	±	0.4
Z+HF	33.5	±	10.3	4.9	±	1.6	4.6	±	1.5
DATA	1889			225			247		
Tot. Exp.	1889.0	±	129.6	225.0	±	18.8	247.0	±	18.4

Table 5: Acceptance table in EwkCR

DRAFT JULY 13, 2010

	1S			SS			SJ		
Top Pair	10.0	±	0.7	1.0	±	0.1	1.4	±	0.2
Single Top	12.7	±	2.2	0.8	±	0.2	1.0	±	0.2
Diboson	10.6	±	1.4	0.3	±	0.1	0.6	±	0.1
Multijet	4570.5	±	274.2	117.8	±	19.2	332.6	±	42.9
W+LF	181.4	±	56.0	0.5	±	0.4	3.7	±	1.4
W+HF	87.8	±	27.0	2.8	±	1.0	5.8	±	1.9
Z+LF	38.3	±	11.8	0.1	±	0.1	0.9	±	0.3
Z+HF	40.7	±	12.6	1.7	±	0.6	3.0	±	1.0
DATA	4952			125			349		
Tot. Exp.	4952.0	±	281.7	125.0	±	19.2	349.0	±	43.0

Table 6: Acceptance table in Lower NN_{QCD} region

	1S			SS			SJ		
Top Pair	22.7	±	1.6	2.1	±	0.2	3.2	±	0.4
Single Top	28.1	±	4.8	2.1	±	0.4	2.6	±	0.5
Diboson	22.5	±	3.0	1.2	±	0.2	1.8	±	0.3
Multijet	1469.7	±	88.2	54.8	±	8.9	91.7	±	11.8
W+LF	193.2	±	59.6	0.9	±	0.5	4.7	±	1.7
W+HF	117.3	±	36.1	5.6	±	1.9	9.0	±	3.0
Z+LF	47.4	±	14.6	0.4	±	0.1	1.3	±	0.4
Z+HF	54.1	±	16.7	3.8	±	1.3	4.8	±	1.6
DATA	1955			71			119		
Tot. Exp.	1955.0	±	114.7	71.0	±	9.2	119.0	±	12.4
SF	1.155	±	0.070	1.371	±	0.224	1.028	±	0.132

Table 7: Acceptance table in Inter NN_{QCD} region

	1S			SS			SJ		
Top Pair	503.4	±	33.4	117.5	±	11.8	102.9	±	11.0
Single Top	195.7	±	33.7	39.0	±	7.5	30.4	±	6.0
Diboson	95.7	±	12.7	13.8	±	2.4	11.5	±	2.0
Multijet	1732.0	±	103.9	93.6	±	15.3	145.1	±	18.7
W+LF	494.7	±	152.2	5.1	±	1.9	17.9	±	6.1
W+HF	405.0	±	124.5	41.7	±	14.1	44.6	±	14.6
Z+LF	155.9	±	47.9	2.6	±	0.9	6.1	±	2.0
Z+HF	184.2	±	56.6	27.6	±	9.1	25.1	±	8.2
DATA	3814			290			401		
Tot. Exp.	3766.6	±	239.5	340.9	±	26.8	383.6	±	28.9

Table 8: Acceptance table in Signal Region

DRAFT JULY 15, 2010

4 $t\bar{t}$ Cross-section Measurement

4.1 Discriminating the signal from remaining backgrounds

In the previous section we described an event selection which enhances the signal purity of the sample by suppressing the presence of backgrounds that do not produce real neutrinos. At this stage of the analysis, the s/b is about 1/6, where the main background processes all produce neutrinos. Unfortunately, the systematic uncertainty on the background prediction is approximately comparable to the size of the signal we seek, depending on the subsample.

Further discrimination of the signal from the background is required. In order to increase the statistical power of the analysis, and to minimize the effect of the background systematic uncertainties, we study the signal sample to take advantage of the small residual differences between the signal and backgrounds. Another neural network will be used for this purpose, where events which appear to be more signal-like are used to measure the cross section, and events which appear to be more background-like are used to constrain the uncertain background rates.

We use the following variables to discriminate between signal and background processes: H_T; $\not{E}_T$; $M(\vec{\not{E}}_T, \vec{j_1}, \vec{j_2})$; the invariant mass of all jets, $M(alljets)$ as shown in Table 4.1. the NN_{QCD} output. The shape comparison plots are shown in Fig 4.

Table 9: Input variables to the neural network aimed at discriminating $t\bar{t}$ production from the backgrounds remaining after the $\mathrm{NN_{QCD}} > -0.5$ requirement.

Variable	Description
H_T	Scalar sum of the jet energies
$\not{E}_T$	Missing transverse energy
$M(\vec{\not{E}}_T, \vec{j_1}, \vec{j_2})$	Invariant mass of $\not{E}_T$, $\vec{j_i}$ and $\vec{j_2}$
$M(alljets)$	Invariant mass of all jets in the event
$QCDNN$	output of the QCD removal NN after the cut $NN_{QCD} > -0.5$

All the above observables are used as inputs to a multi-layer-perceptron neural network trained to distinguish the signal from backgrounds in the sample with $\mathrm{NN_{QCD}} > -0.5$.

The network architecture consists of an input layer with 5 nodes corresponding to the input variables, plus one bias node; one hidden layer with 10 nodes and one hidden layer with 5 nodes, and an output layer with one output node, which we label $\mathrm{NN_{sig}}$. We compare the $\mathrm{NN_{sig}}$ output distribution between the training and testing samples and find good agreement.

DRAFT JULY 15, 2010

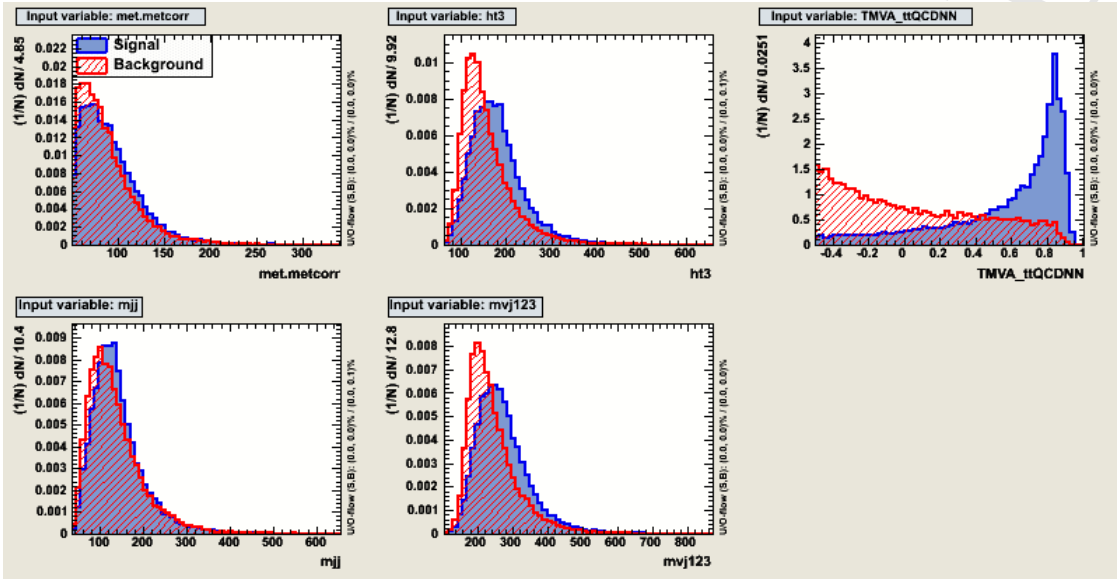

Figure 4: The 5 NN_{sig} inputs in TMVA

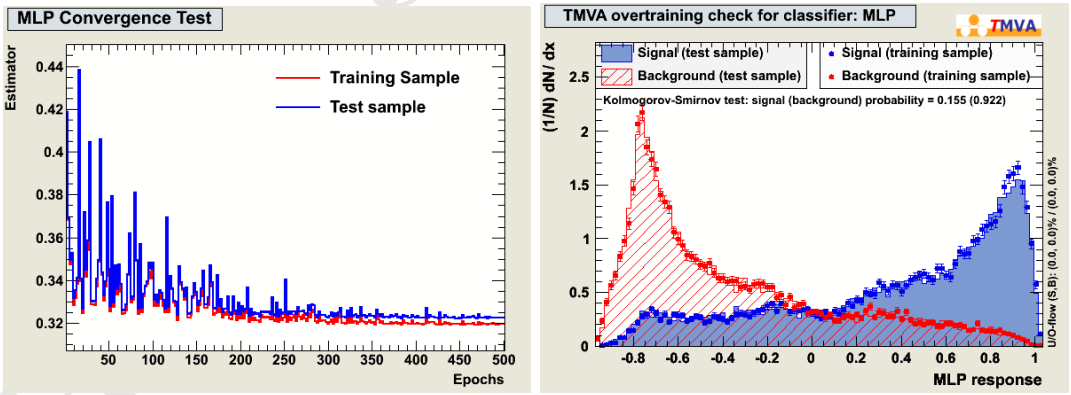

Figure 5: NN_{sig} output, with overtraining check

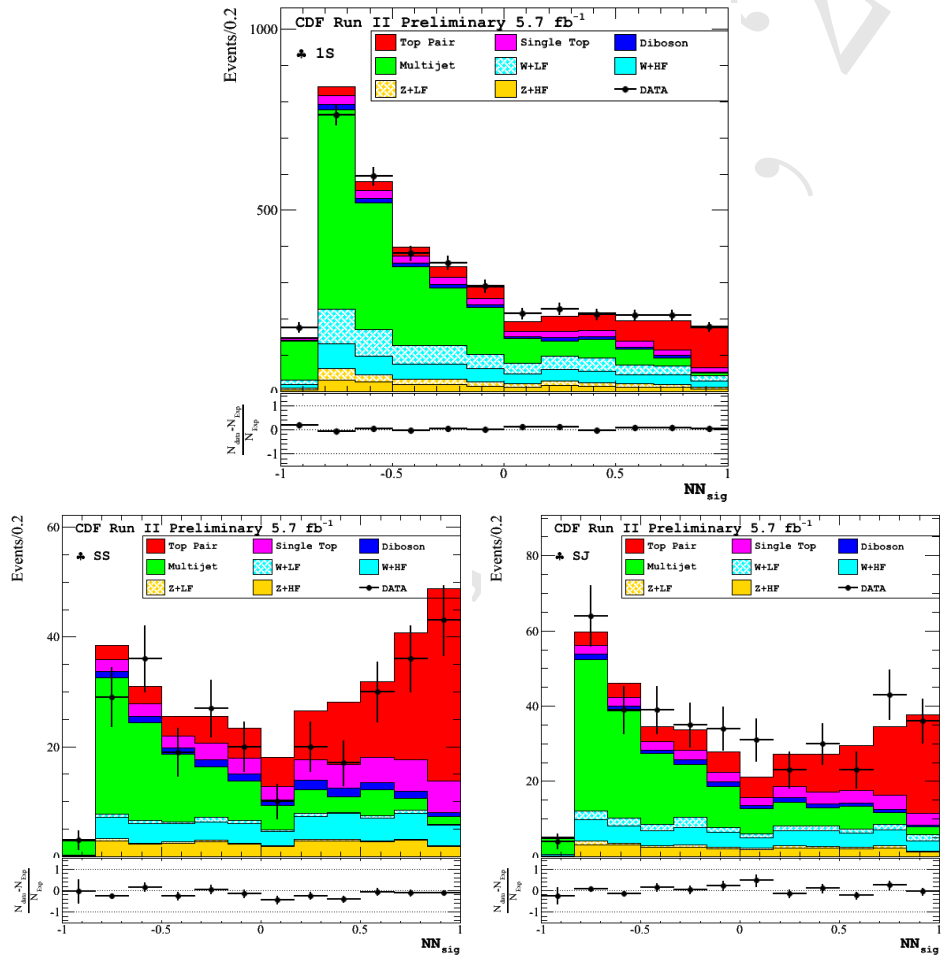

Figure 6: NN_{sig} distribution in signal region, where the multijet scale factor is calculated from the $-0.8 < NN_{QCD} < -0.5$ intermediate region.

DRAFT, 2010

4.2 Systematics

The systematic uncertainties for Monte Carlos:

- Luminosity Uncertainty. The procedure for determining the uncertainty on the luminosity for Run 2 until August 2004 is described in [19]. This uncertainty amounts to 6% and applies to those simulations that are normalized to luminosity.

- PDF Uncertainty. The PDF uncertainty has been determined using the method that is described in [20]. It has been determined that a 2% uncertainty on the acceptance due to the choice of the PDF is sufficient.

- Jet Energy Scale Uncertainty. The Jet Energy Scale uncertainty was determined by varying the jet energy correction factor by plus and minus one sigma while correcting the transverse energy of the jets. This variation then propagates to the $\not\!\!E_T$ reconstruction, the calculation of the azimuthal direction of $\not\!\!E_T$ and thus to the expected number of events after applying the selection cuts. The influence of this variation is different for each background component; therefore, it needs to be determined separately by running the entire analysis code twice on all the simulated backgrounds.

  Since in this analysis we use H1 algorithm to correct jets, additional systematic uncertainties need to be assigned. This is done by varying pT of the tracks used in H1 algorithm by ±3%. The procedure is described in [21]. The uncertainties used in this analysis is shown in Table 10.

JES	1S	SS	SJ
$t\bar{t}$	± 0.8%	± 1.1%	± 1.1%
Single Top	± 4.6%	± 4.7%	± 4.2%
Diboson	± 7.0%	± 8.2%	± 7.0%
W+jets	± 12.7%	± 11.8%	± 7.6%
Z+jets	± 8.3%	± 8.3%	± 7.1%
Multijet	± 5.6%	± 4.0%	± 5.4%

Table 10: Jet energy scale uncertainties. CDF RunII Preliminary L=5.7fb^{-1}

- Lepton Veto. The uncertainty in the efficiency of these cuts were determined to be less than 2%.

- Monte Carlo production cross-section, details has been discussed in Section 2.2.

- B-tagging scale factor. The scale factor for SecVTX and JetProb upto p28 is list in Table 12 [22]. The corresponding systematics uncertainties for 3 tagging categories are shown in Table 13.

DRAFT JULY 15, 2010

Process	XS uncertainty
W+jets	30%
Z+jets	30%
Diboson	11.5%
Single Top s-chan	15.9%
Single Top t-chan	15.2%

Table 11: Uncertainties due to theoretical cross-section predictions

p0-p28	Tight SecVTX	JetProb< 5%
SF	0.96 ± 0.05	0.78 ± 0.05

Table 12: B-tagging scale factor

	1S	SS	SJ
SF error	±5.2%	±7.4%	±8.3%

Table 13: B-tagging scale factor error

- Trigger efficiency uncertainty: we assign a systematic uncertainty to Monte Carlos by varying the trigger efficiency by $\pm 1\sigma$. Table 14 summarizes the uncertainties assigned for each channel in all tagging categories.

Process	1S	SS	SJ
Top Pair	±0.5%	±0.6%	±0.5%
Single Top	±0.8%	±0.9%	±0.8%
Diboson	±0.7%	±1.1%	±0.9%
Multijet	±1.1%	±0.8%	±0.8%
W+jets	±0.9%	±1.0%	±1.0%
Z+jets	±0.7%	±1.0%	±0.7%

Table 14: Uncertainties due to trigger efficiency

Systematics for data-driven multijet model:

- The multijet estimation is based on the Tag Rate Matrix method. This method can well predict multijet shape, and we define an intermediate region ($-0.8 < NN_{QCD} < -0.5$) to derive its scale factor.

$$SF = \frac{data - Exp.\,(MC)\,Signal - Exp.\,MC\,Background}{Multijet\,(before\,SF)} \tag{1}$$

DRAFT JULY 15, 2010

and the uncertainty on scale factor is,

$$\frac{\Delta SF}{SF} = \sqrt{(\frac{\sqrt{data^2_{Err} + \sum MC^2_{Err(stat+sys)_i}}}{data - \sum MC_i})^2 + (\frac{Multijet_{Err}}{Multijet})^2} \quad (2)$$

the calculated scale factor uncertainties are shown in Table 15

	1S	SS	SJ
Multijet SF error	±6.0%	±16.3%	±12.9%

Table 15: Multijet Scale Factor uncertainties

Systematics specified for signal Monte Carlo:

- Color Reconnection: Monte Carlo generators rely on the exact calculation of the perburbative part of the physics of the process, and on phenomenological description of the non-perturbative part. Non-perturbative is for example the color (QCD) connections between final state partons, far away from the time of the interaction, but before hadronization occurs.
- ISR/FSR: The Pythia parameterization of initial and final state radiation (ISR/FSR) is controlled by certain parameters that have uncertainties associate with it [23].
- Herwig: in the Herwid event generator, multiple radiation is treated in the soft or collinear approximation and no emission is permitted in the so-called dead zones, which correspond to hard and large-angle parton radiation.

$t\bar{t}$	1S	SS	SJ
Color Reconnection	±1.6%	±1.9%	±1.5%
ISR/FSR	±2.7%	±4.0%	±1.8%
Herwig	±3.9%	±0.3%	±1.8%

DRAFT JULY 15, 2010

4.3 Likelihood Fit

The cross-section of $t\bar{t}$ production is measured by fitting $\mathrm{NN_{sig}}$ distribution in the data to a sum of signal and background templates. The tool we are using is MCLIMIT.

The likelihood fit is applied to each pseudo-experiment to calculate fitted β and its asymmetric uncertainties σ^+ and σ^-, where

$$\beta = \frac{measured\,cross\,section}{input\,cross\,section} \tag{3}$$

To cross-check the fitter performance, we had several approaches:

- We expect the measured β is well distributed around the expected β. So we checked the pull distribution.

$$pull = \begin{cases} \frac{\beta_{exp}-\beta_{meas}}{\sigma^+}, & \beta_{meas} \leq \beta_{exp} \\ \frac{\beta_{meas}-\beta_{exp}}{\sigma^-}, & \beta_{meas} > \beta_{exp} \end{cases} \tag{4}$$

  By running with 6500 pseudo-experiments, and with 100000 systematics samples, the pull distribution is shown in Fig. 7.

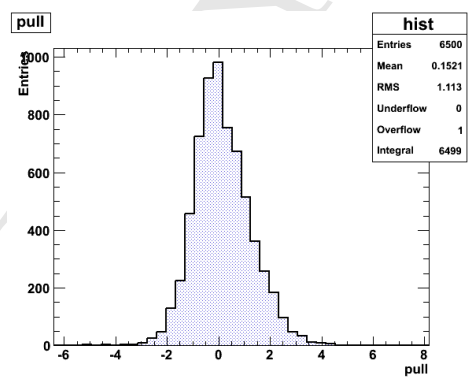

Figure 7: Pull distribution, include all of the introduced systematics.

- Linearity test: by moving the input cross-section in a range (0pb $\sim$ 15pb), to check the performance of measured cross-section. By moving in 9 steps, a nice agreement is shown in Fig 8.

- We also measured the β for the other backgrounds: treat each individual background as signal.

DRAFT - May 15, 2010

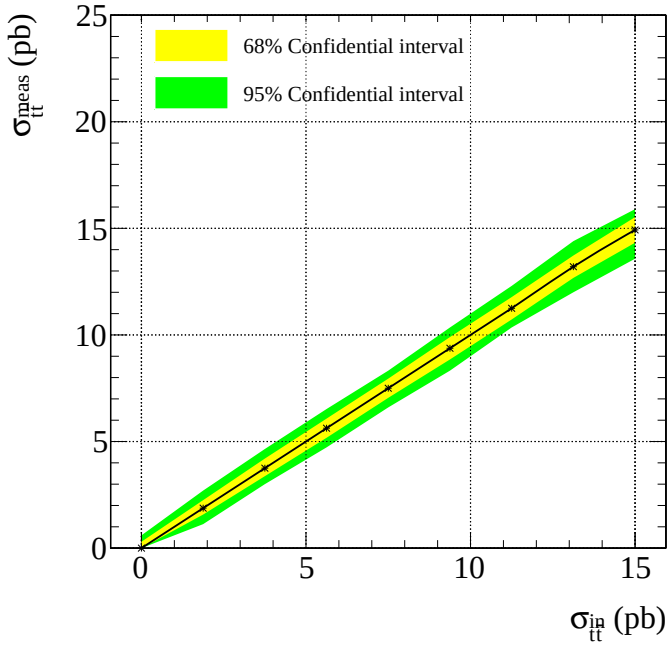

Figure 8: Linearity of the fitted cross-section as a function of input cross-section in pseudo-experiments. Only statistics have been included in this performance check.

Process	-2σ	$-\sigma$	β	$+\sigma$	$+2\sigma$
Multijet	0.93	0.96	1	1.04	1.07
W+Jets	0.88	0.94	1	1.06	1.12
Z+Jets	0.69	0.86	1.01	1.14	1.31
Single Top	0.47	0.71	1	1.27	1.56
Diboson	0	0.44	0.97	1.46	1.99

Table 16: Expected β and its uncertainties for other backgrounds. Only statistics have been included in this performance check.

DRAFT JUL 2010

4.4 Results

In the signal region, by using the NN_{Sig}, our sensitivities are shown in Table 17.

	1S	SS	SJ
$\sqrt{\sum \frac{S_i}{(S+B)_i}}$	12.3	7.5	6.6

Table 17: Sensitivity of signal region, using NN_{Sig}

With statistics only,

- The expected cross-section: $\sigma_{t\bar{t}} = 7.50^{+0.53}_{-0.45}\,(stat.)\,pb$
- The observed cross-section: $\sigma_{t\bar{t}} = 6.75^{+0.45}_{-0.53}\,(stat.)\,pb$

With the systematics,

- The expected cross-section: $\sigma_{t\bar{t}} = 7.43^{+1.20}_{-1.13}\,(stat. + syst.)\,pb$
- The observed cross-section: $\sigma_{t\bar{t}} = 7.12^{+1.20}_{-1.12}\,(stat. + syst.)\,pb$

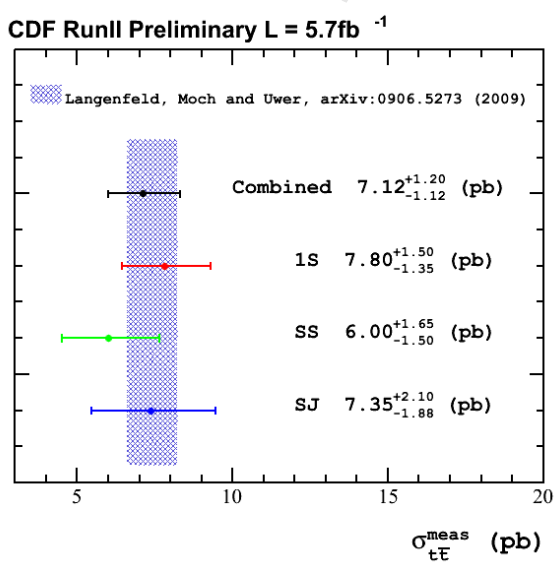

DRAFT July 15, 2010

5 Summary

In conclusion we report the first measurement of the top pair production cross section of $\sigma_{t\bar{t}} = 7.05^{+0.98}_{-0.75}\,(stat. + syst.)\,pb$ using an exclusive selection of MET+2/3jets decays, analyzing $\int Ldt = 5.7\,fb^{-1}$ data. The result is complementary to other cross section analyses, maintains high sensitivity with respect to $W \to \tau\nu$ decays, and is in good agreement with SM calculations and previous measurements.

References

[1] A. Abulencia *et al.* [CDF Collaboration], "Measurement of the t anti-t production cross section in $p\bar{p}$ collisions at $sqrts = 1.96$-TeV using missing E(t) + jets events with secondary vertex b-tagging," Phys. Rev. Lett. **96** (2006) 202002

[2] G. Compostella, S. Amerio, D. Lucchesi, "Measurement of the ttbar production cross section in the MET+jets channel in 2.2 fb-1" CDF conference note 9988;

[3] D. Bortoletto, Q. Liu, F. Margaroli, K. Potamianos, O. Gonzalez, M. Vidal "Search for the Standard Model Higgs boson in the MET plus jets sample" CDF Note 10166;

[4] T. Aaltonen *et al.* [CDF Collaboration], "Observation of Electroweak Single Top Quark Production," Phys. Rev. Lett. **103** (2009) 092002;

[5] T. Aaltonen *et al.* [The CDF Collaboration], "Search for single top quark production in pbar p collisions at sqrts=1.96 TeV in the missing transverse energy plus jets topology," Phys. Rev. D **81** (2010) 072003;

[6] Q. Liu, F.Margaroli "Everything you wanted to know on the missing transverse momentum from the tracker" CDF Note 9843;

[7] Z. Sullivan, Phys. Rev. D **70**, 114012 (2004).

[8] B.W. Harris *et al.*, Phys. Rev. D **66**, 054024 (2002).

[9] J. M. Campbell and R. K. Ellis, Phys. Rev. D **62**, 114012 (2000).

[10] J. M. Campbell and R. K. Ellis, Phys. Rev. D **60**, 113006 (1999).

[11] A momentum tensor is defined as $M_{lm} = \frac{\sum_o j_l^o j_m^o}{\sum_o |\vec{j^o}|}$, where $\vec{j^o}$ is the momentum of a reconstructed jet, and l and m are Cartesian coordinates. The index o runs over the number of jets in the event. The sphericity in an event is defined as $S = \frac{3}{2}(\lambda_2 + \lambda_3)$, where λ_2 and λ_3 are the smallest two eigenvalues of the normalized momentum tensor.

DRAFT JULY 15, 2010

[12] A. Apresyan, D. Bortoletto, F. Margaroli, O. Gonzalez, M. Vidal, S.M. Wang, "Tag Rate Matrix method to estimate QCD background fromdata in VH search in MET + b-jets signature", CDF Note 9275;

[13] O. Gonzalez and M. Vidal, "Getting ready for the 4 fb-1 dataset: Trigger efficiency of the MET+JETS samples" CDF Note 9745;

[14] O. Gonzalez and M. Vidal, "Official Recovery of Events with Saturated Towers using the JET-100 sample (for the MET dataset)" CDF Note 9231;

[15] A. Castro, F. Margaroli [CDF Collaboration], Phys. Rev. D **76** (2007) 072009 [arXiv:0706.3790 [hep-ex]];

[16] L. Brigliadori, A. Castro, F. Margaroli [The CDF Collaboration], "Measurement of the Top Quark Mass and $p\bar{p} \to t\bar{t}$ Cross Section in the All-Hadronic Mode with the CDFII Detector,"a Phys. Rev. D **81** (2010) 052011;

[17] Tevatron Electroweak Working Group, CDF and D0 Collaborations, "Combination of CDF and D0 Results on the Mass of the Top Quark," arXiv:0903.2503;

[18] P. Z. Skands, "The Perugia Tunes," arXiv:0905.3418;

[19] S. Jindariani et al., "Luminosity Uncertainty for Run 2 up until August 2004," CDF Note 7446, 2005;

[20] O. Gonzalez, C. Rott, "Uncertainties due to the PDFs for the gluino-sbottom search," CDF Note 7051, 2004;

[21] A. Mehta, "Calibration of H1 Algorithm Improved Jets," CDF Note 8564, 2006;

[22] V. Giakoumopoulou, J. Freeman, "Summer 2010 SevVtx Scale Factors Calculated Using the Electron Method through Period 28," CDF Note 10178, 2010;

[23] Young-kee Kim, Un-ki Yang, "Initial state gluon radiation studies on Drell-Yan data for top-pair production in hadron collider," CDF Note 6804, 2003;

DRAFT JULY 15, 2010

A Lepton Identification

Table 18: Loose Lepton ID

Central Electron	
Et	≥ 20
E/P	< 4
Had/Em	< 0.125
Lshr	< 0.2
DeltaX	< 3
DeltaZ	< 5
Iso4	< 0.2
chi2	$< 10.$

Plug Electron	
Et	≥ 20
Had/Em	< 0.125
chi2	$< 10.$

Muon	
Pt	≥ 20
EM energy	< 2
HD energy	< 6
Isolation	< 0.1
Z0	< 60
COTAx(5hits)	≥ 3
COTSt(5hits)	≥ 2

DRAFT JULY 15, 2010

B Tag Rate Matrix

Tag Rate Matrix is a data-based method to estimate the multijet tagging probability. In a QCD dominant region, we build up a 4D matrix to calculate b-tag rate, as shown in Table 19.

J1(2)Et	25	50	80	100	120	150	200	1000
J1(2)$\|\eta\|$	0.0	0.4	0.8	2.0				
HT3	60	150	350	1000				
J1(2)Z	0.0	0.05	0.1	0.2	0.4	0.8	10.	

Table 19: 4D matrix based on jet information

In each 4D matrix bin, we calculate the b-tag rate (R_{1S}, R_{SS}, R_{SJ}):

$$R_{1S} = \frac{\#Events\ falling\ into\ bin\ i_{single\ SecVTX\ tagged}}{\#jets\ falling\ into\ bin\ i_{SecVTX\ taggable}} \tag{5}$$

$$R_{SS} = P_{1S_{J1}} \times P_{1S_{J2}} \tag{6}$$

$$R_{SJ} = \frac{1}{2} \times (P_{1S_{J1}} \times P_{1J_{J2}} + P_{1J_{J1}} \times P_{1S_{J2}}) \tag{7}$$

where,

$$P_{1S} = \frac{\#1^{st}jets_{SecVTX\ tagged} + \#2^{nd}jets_{SecVTX\ tagged}}{\#1^{st}jets_{SecVTX\ taggable} + \#2^{nd}jets_{SecVTX\ taggable}} \tag{8}$$

$$P_{1J} = \frac{\#1^{st}jets_{JetProb\ tagged} + \#2^{nd}jets_{JetProb\ tagged}}{\#1^{st}jets_{JetProb\ taggable} + \#2^{nd}jets_{JetProb\ taggable}} \tag{9}$$

- Apply Tag Rate Matrix
  - In each region, we apply the Tag Rate Function both to the data and Monte Carlos. For example, to estimate 1S multijet, we use,

    $$Multijet = (data \times R_{1S} - \sum Monte\,Carlo_i \times R_{1S}) \times f_{scale} \tag{10}$$

    a f_{scale} is introduced due to that the multijet model can predict the shape of tagged multijet very well, but lack the ability to precisely predict amount of multijet.
  - We also define a control region to predict the f_{scale} for signal region
- Validate Tag Rate Matrix
  - We define several control region to validate this data-driven model
  - details will be discussed after introducing the methods to define control/signal regions.

DRAFT JULY 15, 2010

C Validation Plots

DRAFT JULY 15, 2010

C.1 TRM

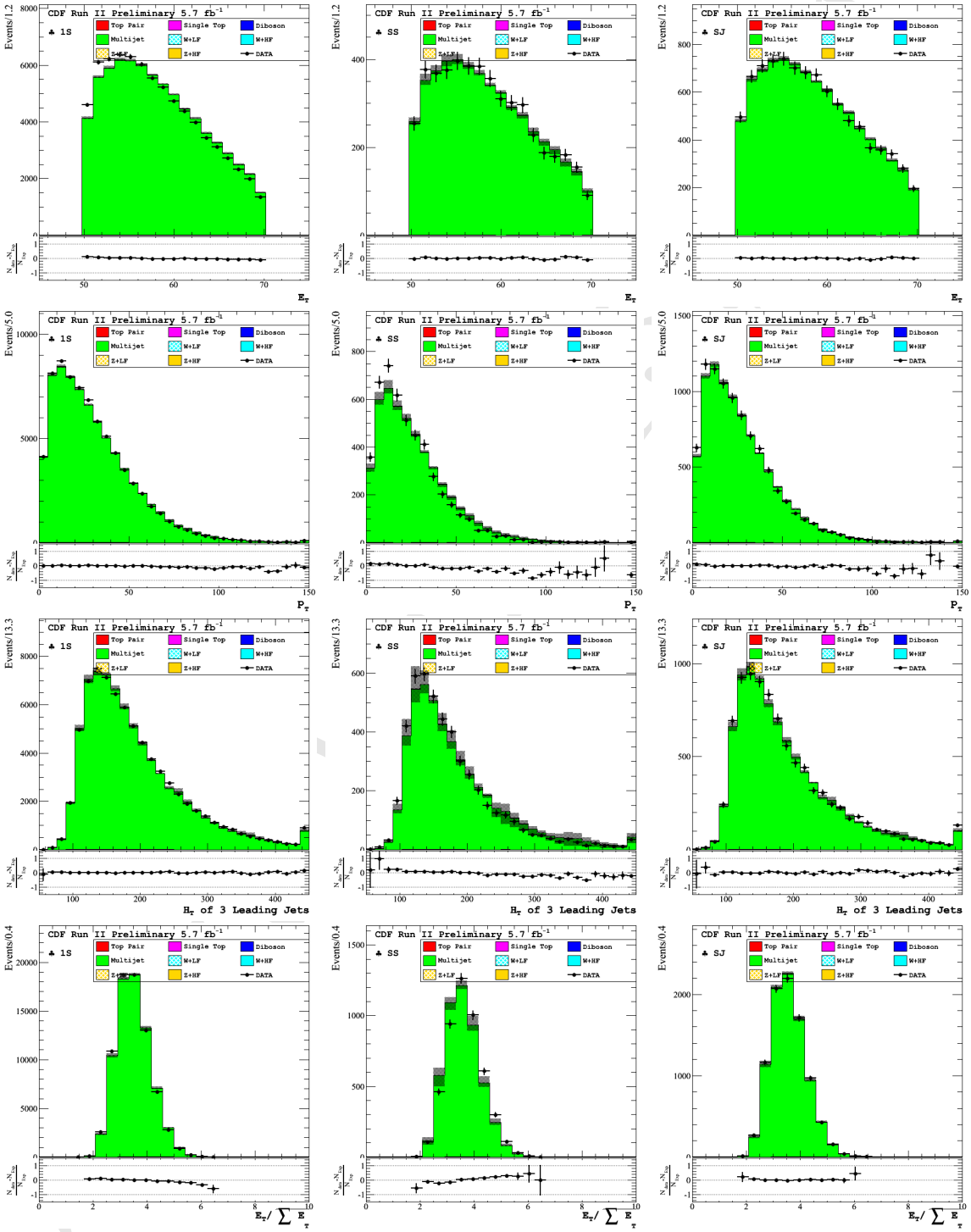
CDF Run II Preliminary 5.7 fb^{-1}
1S
SS
SJ
Top Pair
Single Top
Diboson
Multijet
W+LF
W+HF
Z+LF
Z+HF
DATA
Events/1.2
Events/5.0
Events/13.3
Events/0.4
E_T
P_T
H_T of 3 Leading Jets
$E_T/\sum E_T$
$N_{data}-N_{bg}$ / N_{bg}

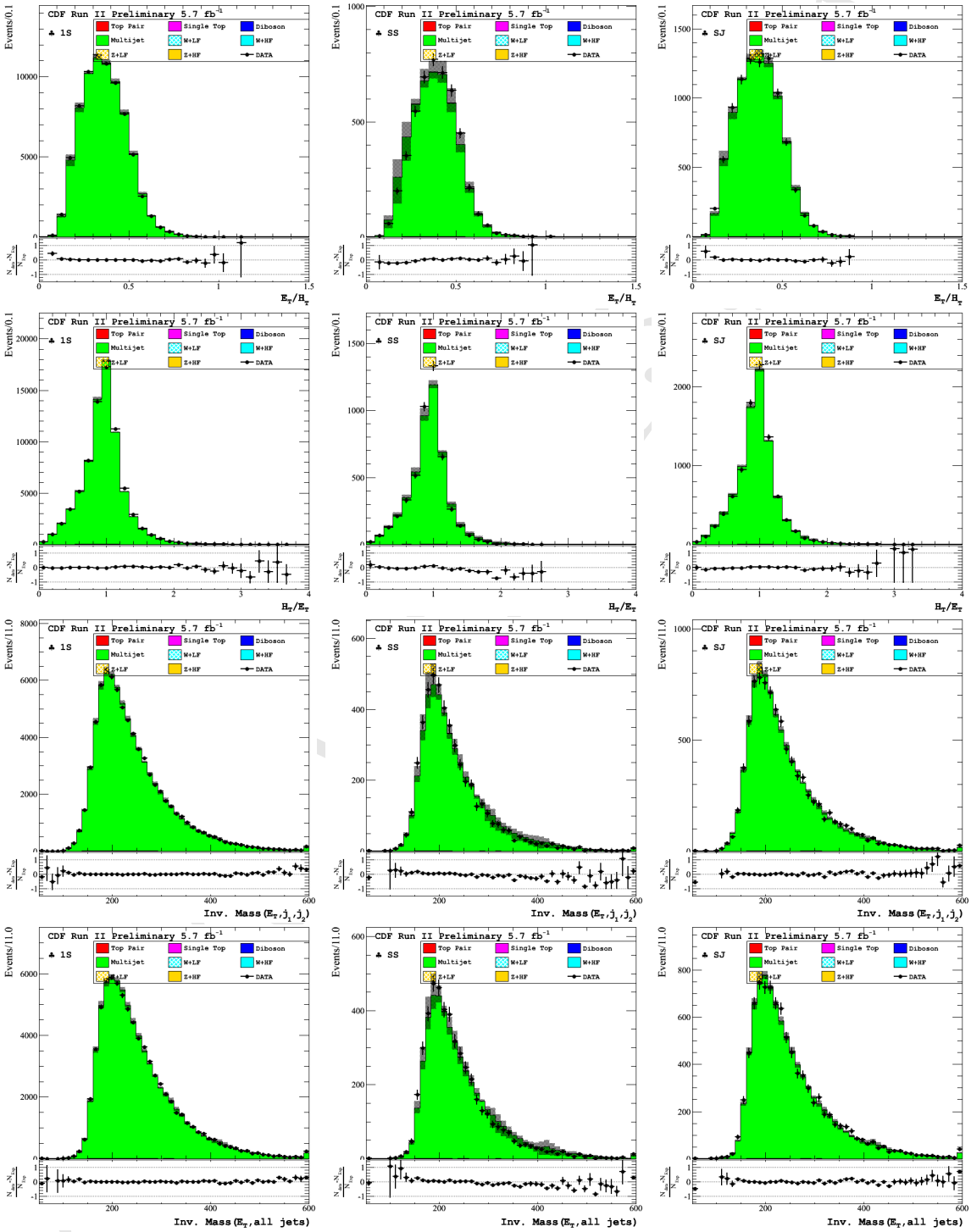
CDF Run II Preliminary 5.7 fb^{-1}
1S
SS
SJ
Top Pair
Single Top
Diboson
Multijet
W+LF
W+HF
Z+LF
Z+HF
DATA
Events/0.1
Events/1.0
E_T/H_T
H_T/E_T
Inv. Mass(E_T,j_1,j_2)
Inv. Mass(E_T,all jets)
$N_{data}-N_{bg}$ / N_{bg}

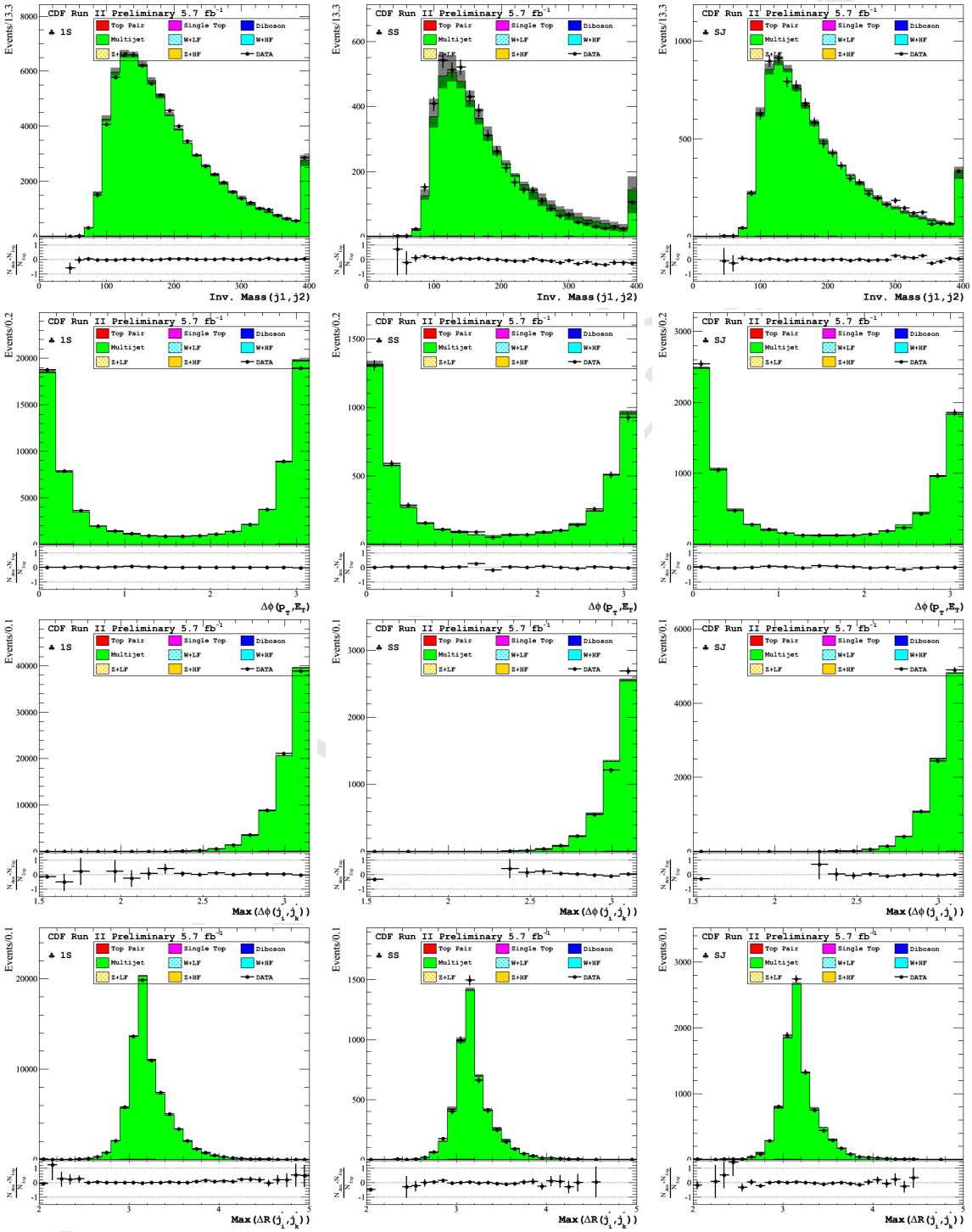
CDF Run II Preliminary 5.7 fb^{-1}
1S
SS
SJ
Top Pair
Single Top
Diboson
Multijet
W+LF
W+HF
Z+LF
Z+HF
DATA
Events/13.3
Inv. Mass(j1,j2)
Events/0.2
$\Delta\phi(p_T, E_T)$
Events/0.1
Max($\Delta\phi(j_i, j_k)$)
Max($\Delta R(j_i, j_k)$)
$N_{data}-N_{bg}$ / N_{bg}

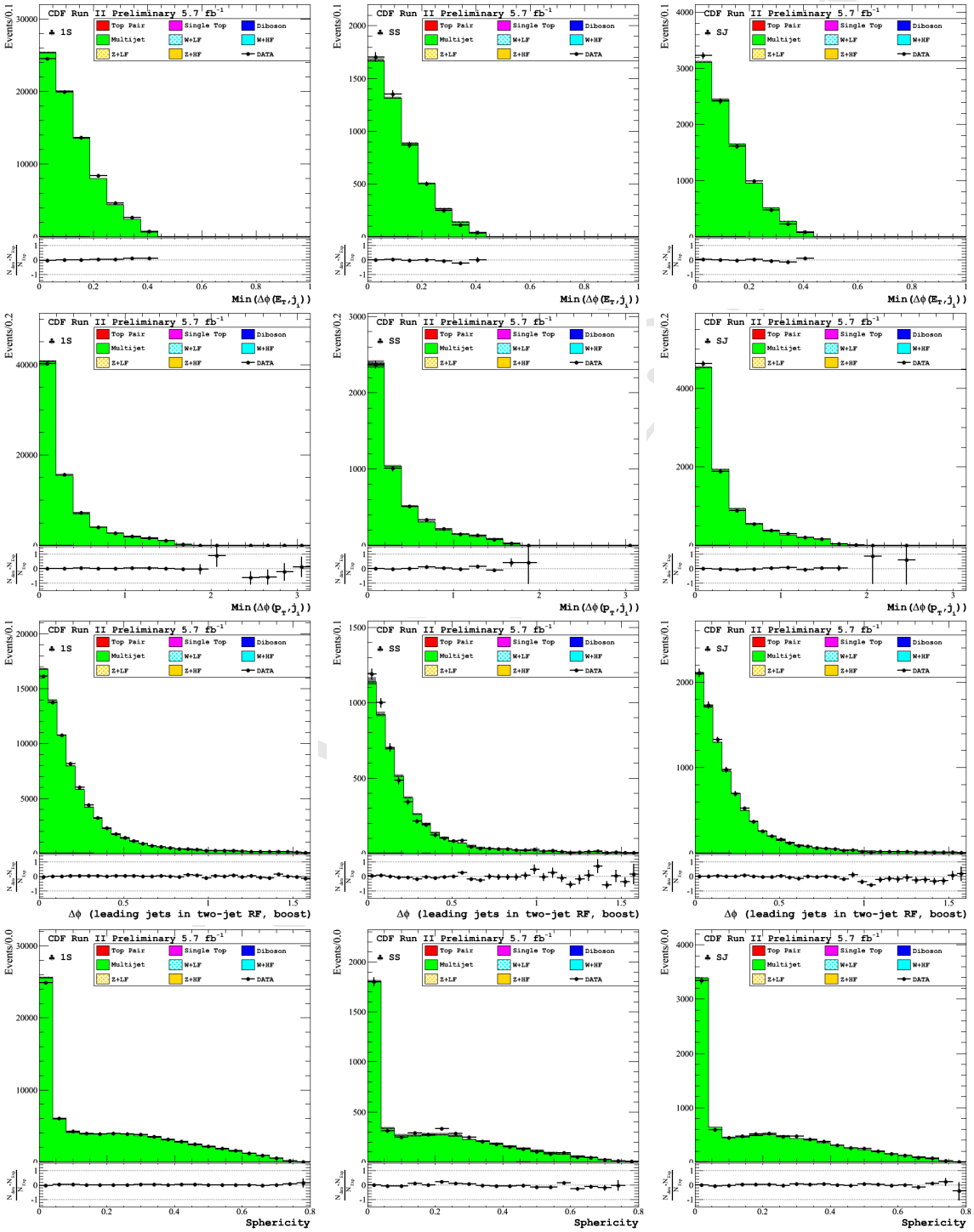
CDF Run II Preliminary 5.7 fb^{-1}
1S
SS
SJ
Top Pair
Single Top
Diboson
Multijet
W+LF
W+HF
Z+LF
Z+HF
DATA
Events/0.1
Events/0.2
Events/0.0
Min($\Delta\phi(\not{E}_T, j_1)$)
Min($\Delta\phi(\not{p}_T, j_1)$)
$\Delta\phi$ (leading jets in two-jet RF, boost)
Sphericity
$N_{Bg}-N_{Dis}$ / N_{Tot}

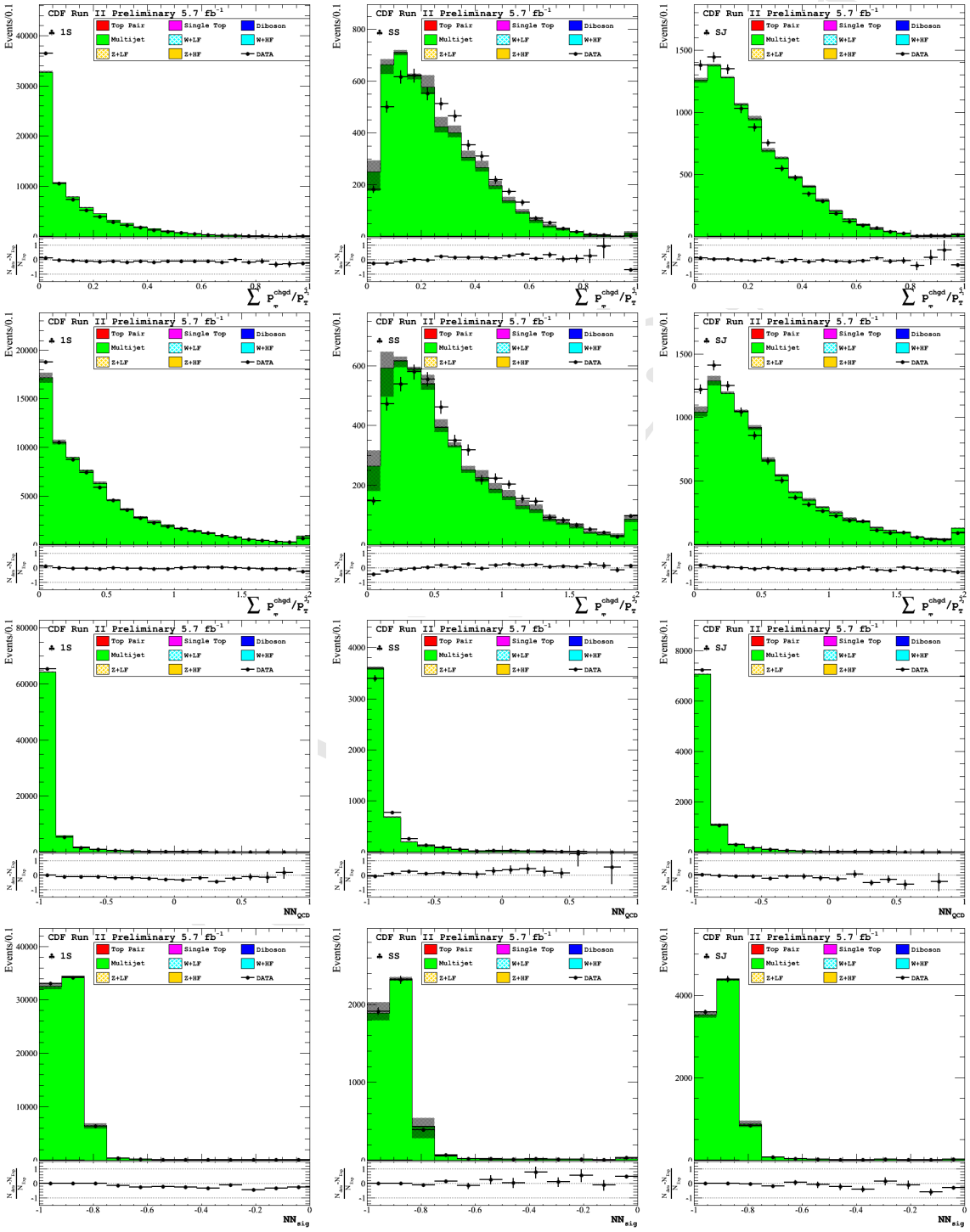
CDF Run II Preliminary 5.7 fb^{-1}
1S
SS
SJ
Top Pair
Single Top
Diboson
Multijet
W+LF
W+HF
Z+LF
Z+HF
DATA
Events/0.1
$\sum p_{\pi}^{chgd}/p_{\tau}^{1-1}$
$\sum p_{\pi}^{chgd}/p_{\tau}^{1-2}$
NN_{QCD}
NN_{sig}
$N_{data}-N_{bg}$ / N_{tot}

C.2 QCDCR

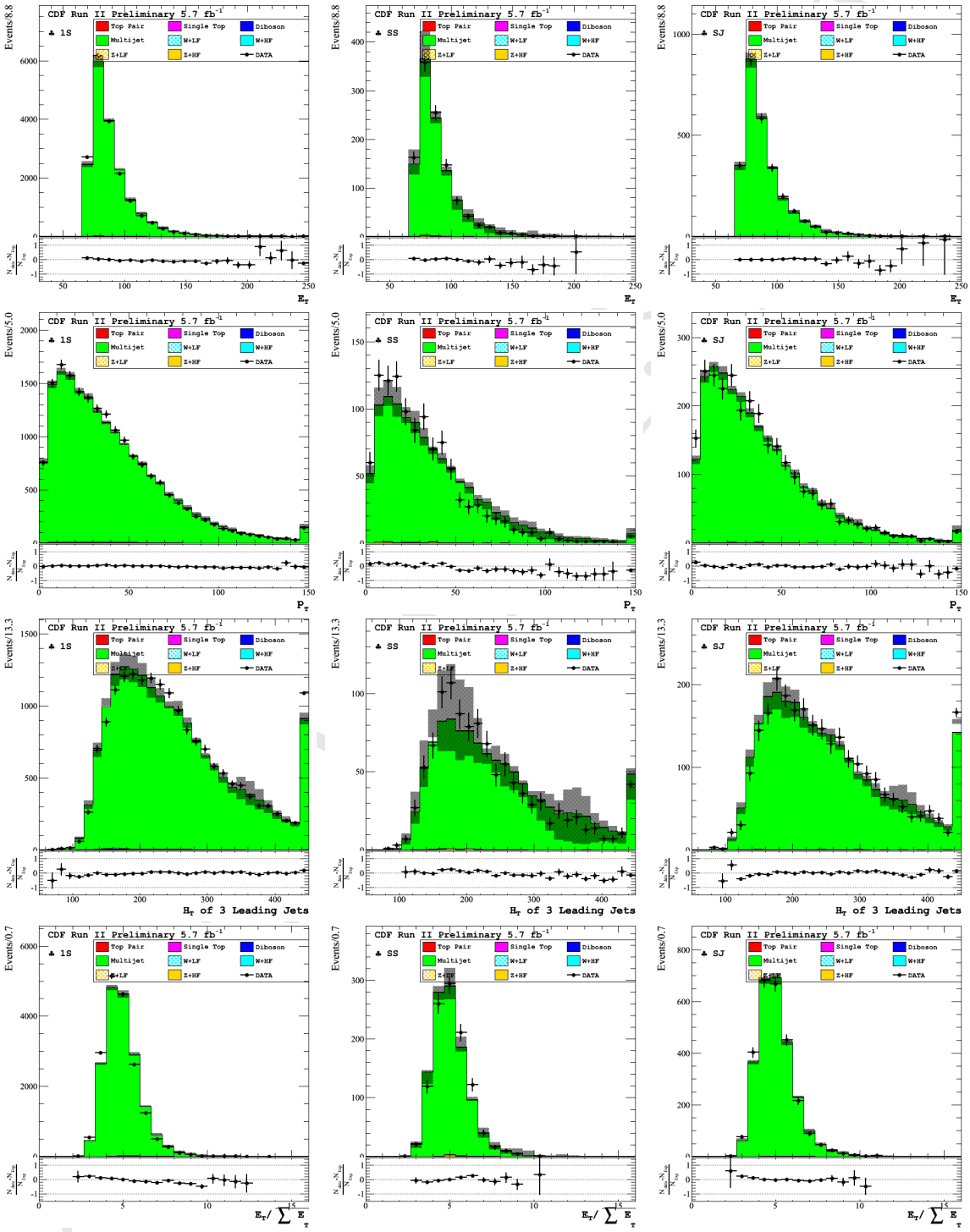
CDF Run II Preliminary 5.7 fb^{-1}
1S
SS
SJ
Top Pair
Single Top
Diboson
Multijet
W+LF
W+HF
Z+LF
Z+HF
DATA
Events/8.8
Events/5.0
Events/13.3
Events/0.7
E_T
P_T
H_T of 3 Leading Jets
$E_T/\sum E_T$
$\frac{N_{data}-N_{bg}}{N_{bg}}$

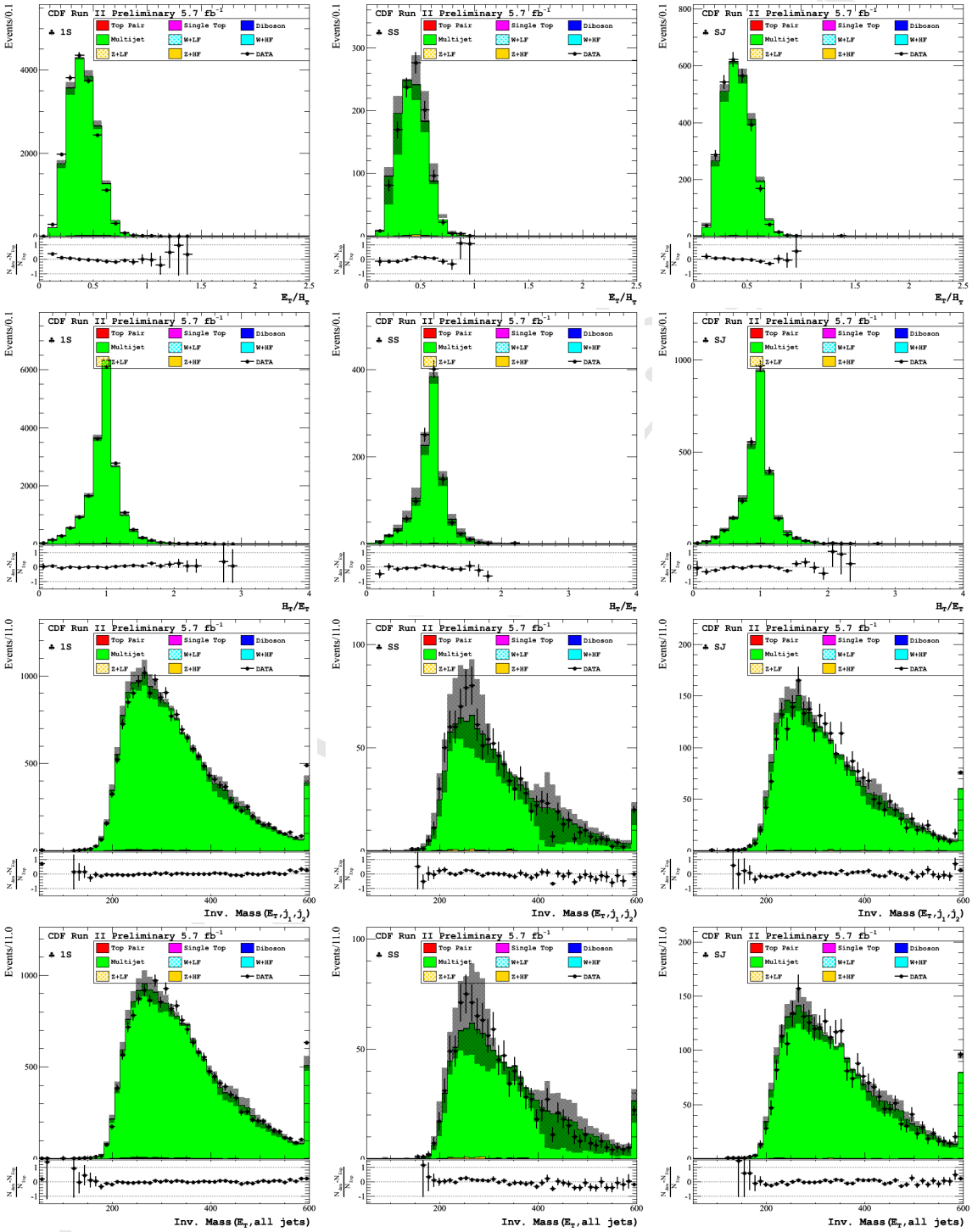
CDF Run II Preliminary 5.7 fb^{-1}
1S
SS
SJ
Top Pair
Single Top
Diboson
Multijet
W+LF
W+HF
Z+LF
Z+HF
DATA
Events/0.1
Events/11.0
E_T/H_T
H_T/E_T
Inv. Mass(E_T,j_1,j_2)
Inv. Mass(E_T,all jets)
$N_{data}-N_{bg}$ / N_{bg}

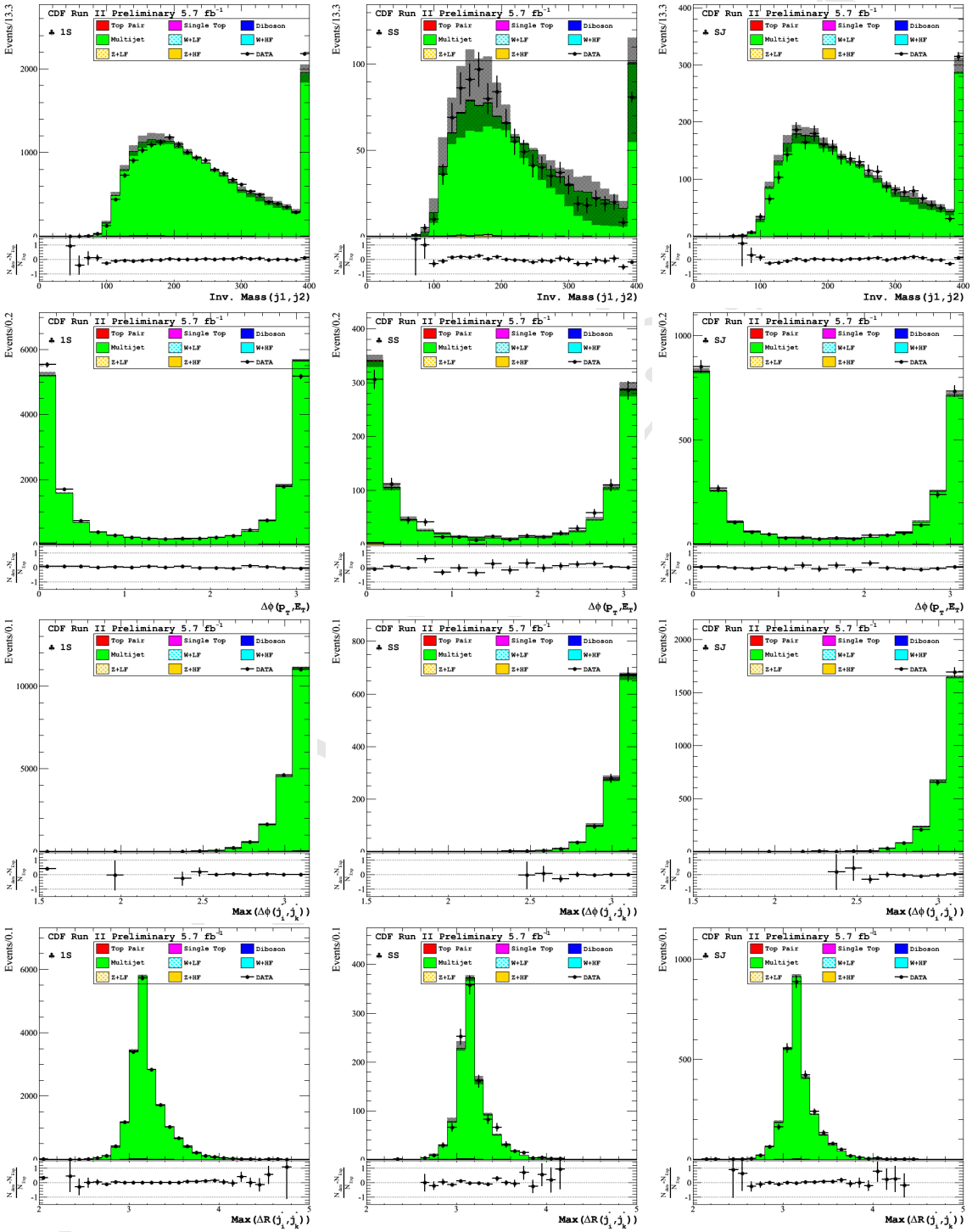
CDF Run II Preliminary 5.7 fb^{-1}
1S
SS
SJ
Top Pair
Single Top
Diboson
Multijet
W+LF
W+HF
Z+LF
Z+HF
DATA
Events/13.3
Inv. Mass(j1,j2)
Events/0.2
$\Delta\phi(p_T, E_T)$
Events/0.1
Max($\Delta\phi(j_i, j_k)$)
Max($\Delta R(j_i, j_k)$)
$N_{data}-N_{bg}$ / N_{bg}

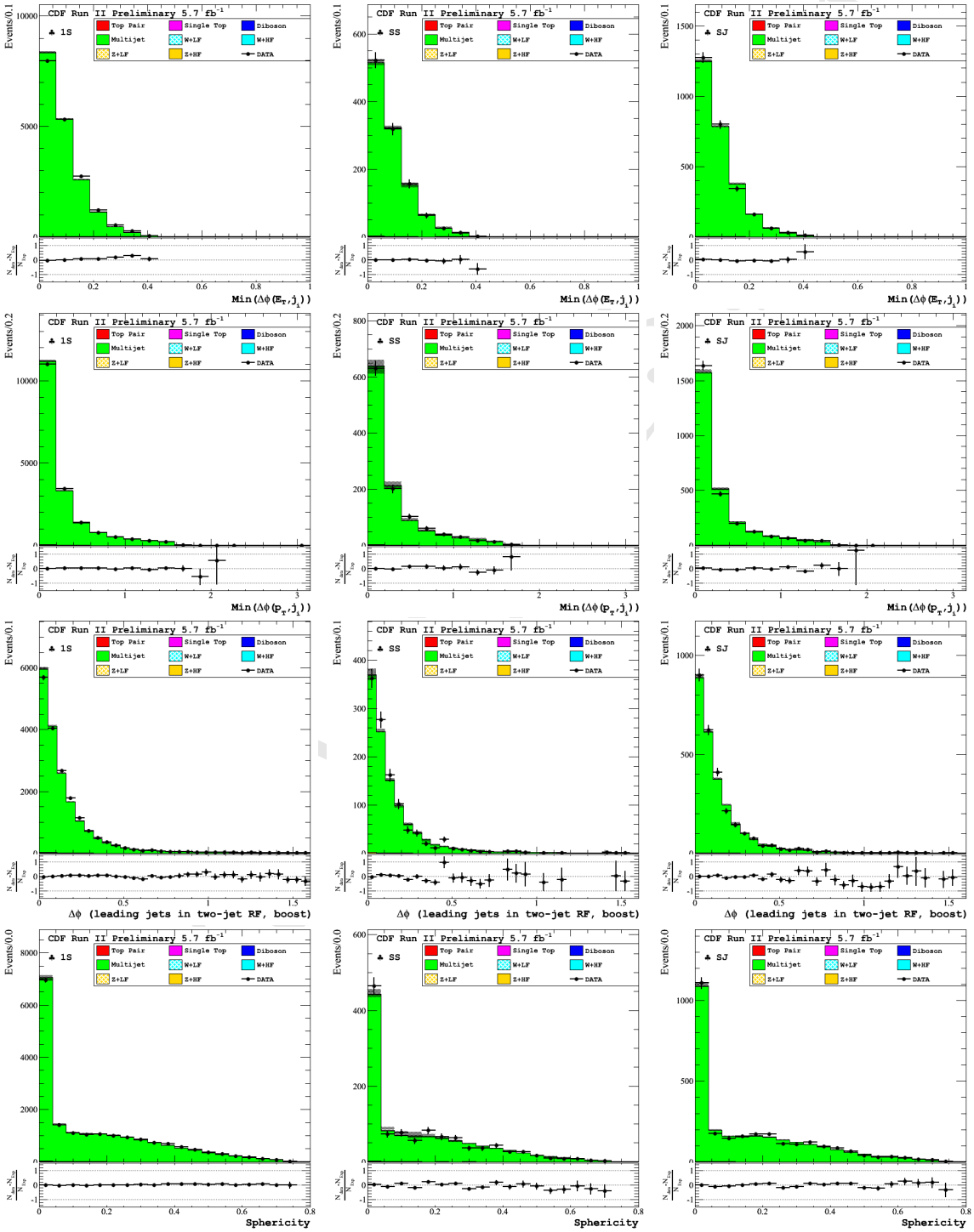
CDF Run II Preliminary 5.7 fb^{-1}
1S
SS
SJ
Top Pair
Single Top
Diboson
Multijet
W+LF
W+HF
Z+LF
Z+HF
DATA
Events/0.1
Events/0.2
Events/0.0
Min($\Delta\phi(\not{E}_T, j_1)$)
Min($\Delta\phi(\not{p}_T, j_1)$)
$\Delta\phi$ (leading jets in two-jet RF, boost)
Sphericity
$\frac{N_{Bkg}-N_{Data}}{N_{Bkg}}$

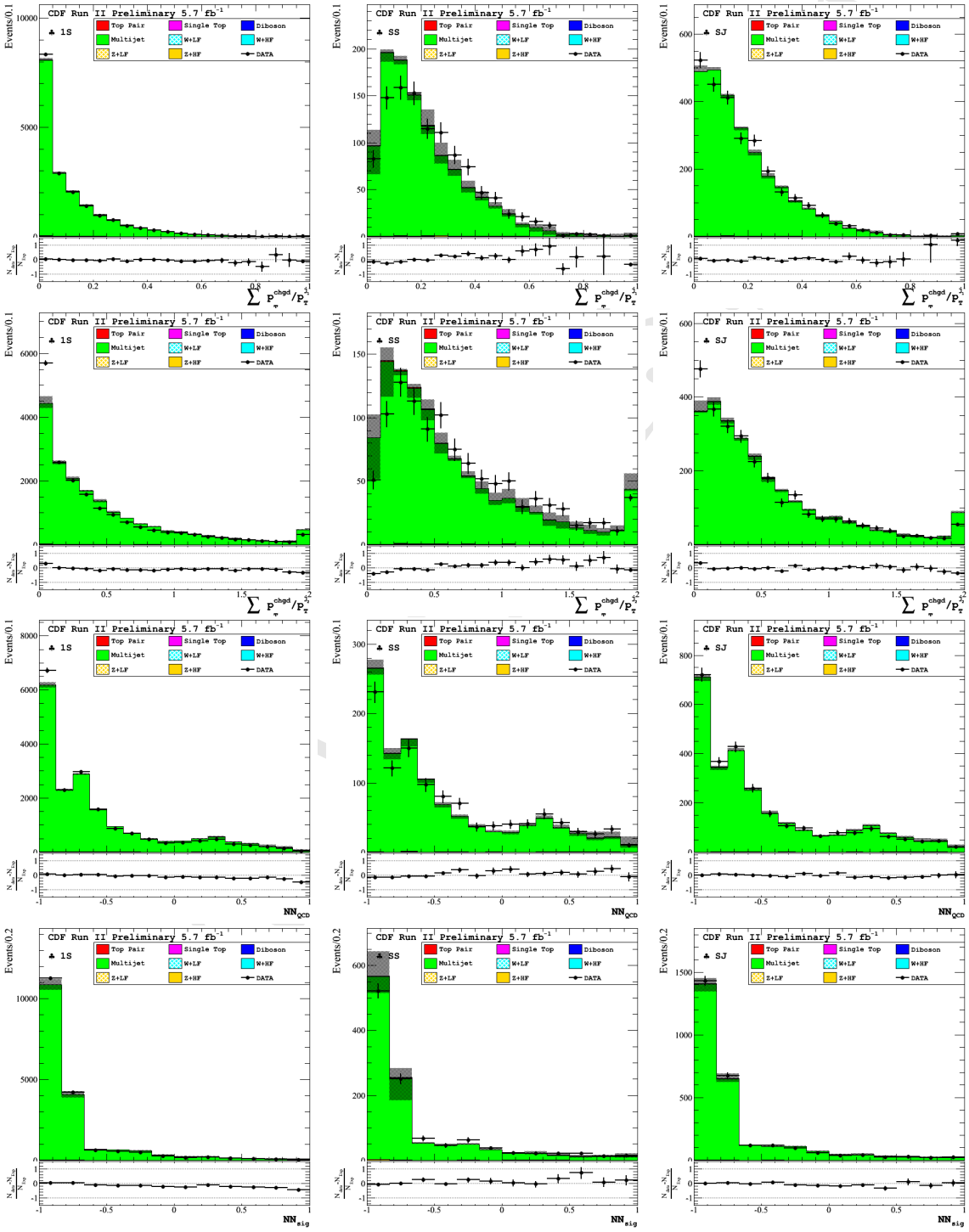
CDF Run II Preliminary 5.7 fb^{-1}
1S
SS
SJ
Top Pair
Single Top
Diboson
Multijet
W+LF
W+HF
Z+LF
Z+HF
DATA
Events/0.1
Events/0.2
$\sum p_{\pi}^{chgd}/p_{\tau}^{jet}$
NN_{QCD}
NN_{sig}
$N_{data}-N_{bg}$ / N_{tot}

C.3 EwkCR

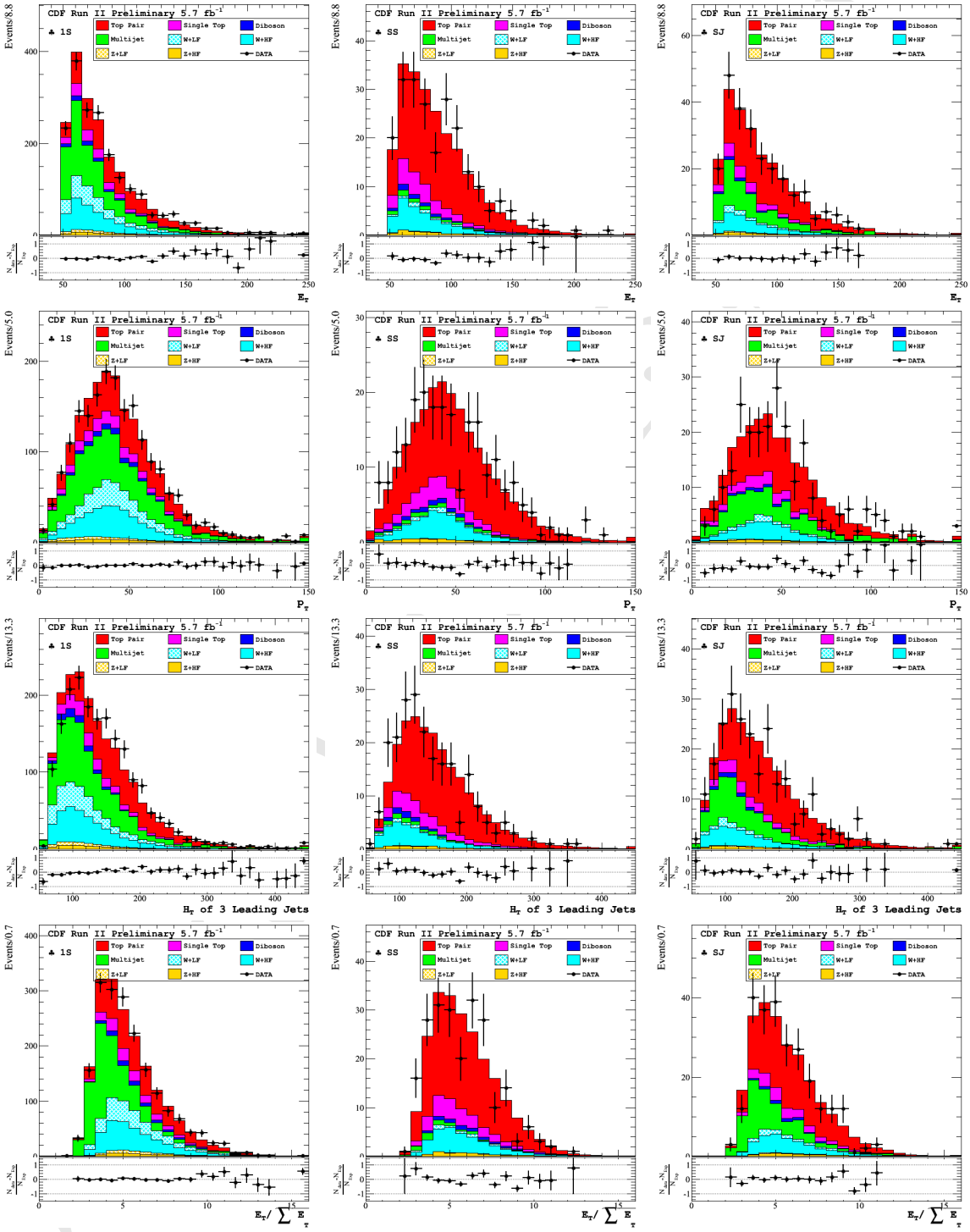
CDF Run II Preliminary 5.7 fb^{-1}
1S
SS
SJ
Top Pair
Single Top
Diboson
Multijet
W+LF
W+HF
Z+LF
Z+HF
DATA
Events/8.8
Events/5.0
Events/13.3
Events/0.7
E_T
P_T
H_T of 3 Leading Jets
$E_T/\sum E_T$

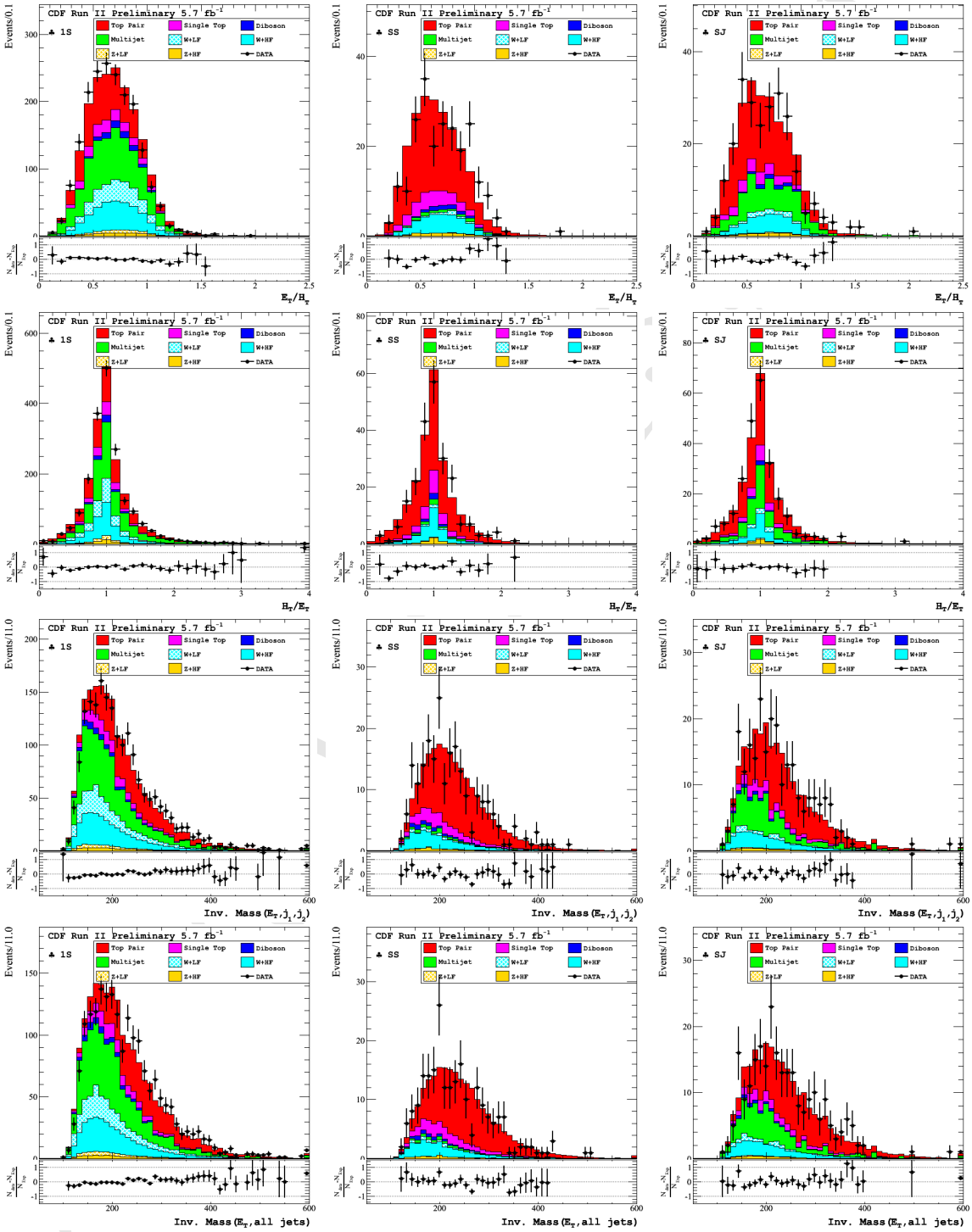
CDF Run II Preliminary 5.7 fb^{-1}
1S
SS
SJ
Top Pair
Single Top
Diboson
Multijet
W+LF
W+HF
Z+LF
Z+HF
DATA
Events/0.1
Events/11.0
E_T/H_T
H_T/E_T
Inv. Mass(E_T,j_1,j_2)
Inv. Mass(E_T,all jets)
$N_{data}-N_{bg}$ / N_{bg}

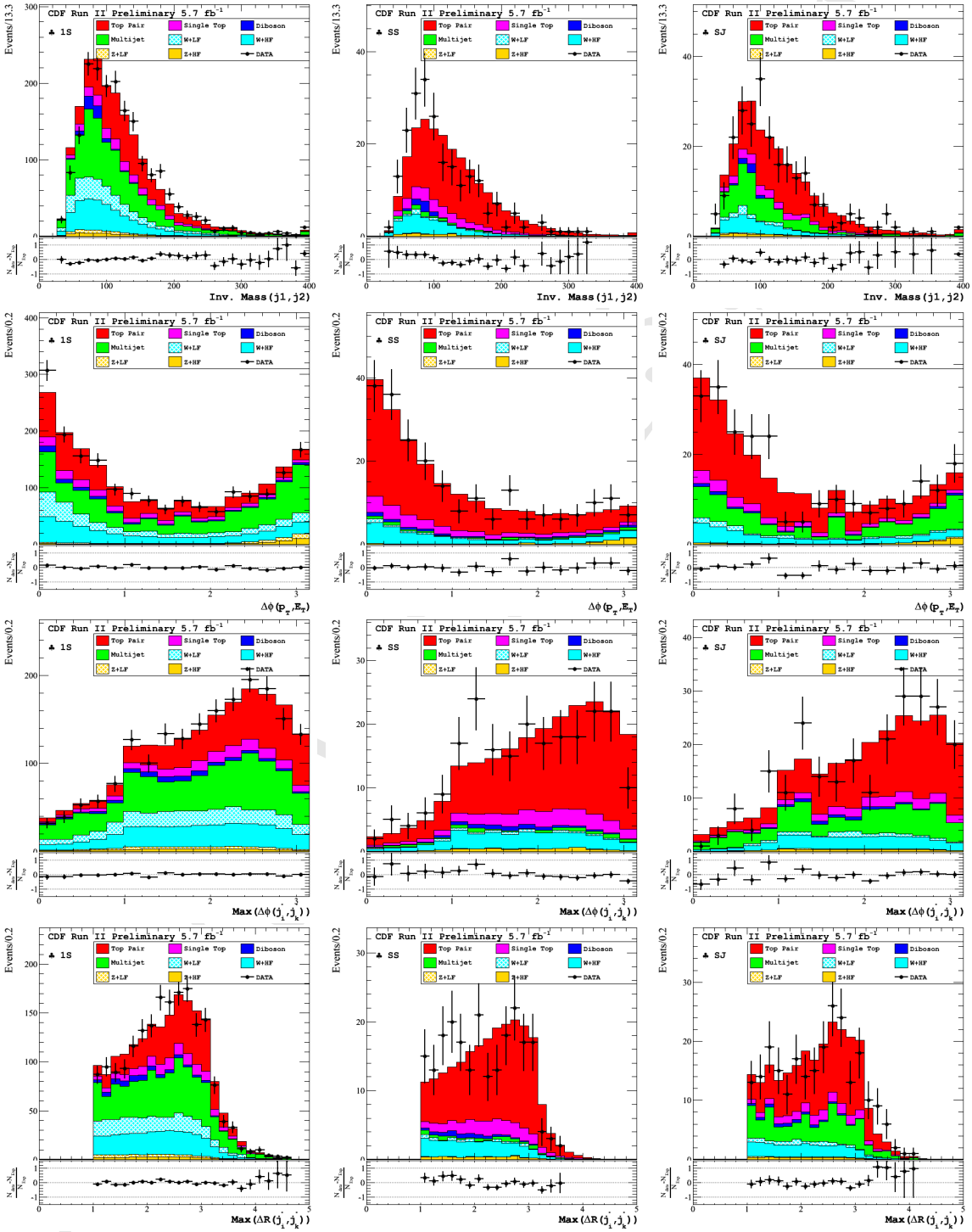
CDF Run II Preliminary 5.7 fb^{-1}
1S
SS
SJ
Top Pair
Single Top
Diboson
Multijet
W+LF
W+HF
Z+LF
Z+HF
DATA
Events/13.3
Events/0.2
Inv. Mass(j1,j2)
$\Delta\phi(\not{p}_T,\not{E}_T)$
Max($\Delta\phi(j_i,j_k)$)
Max($\Delta R(j_i,j_k)$)
$N_{data}-N_{bg}$ / N_{bg}

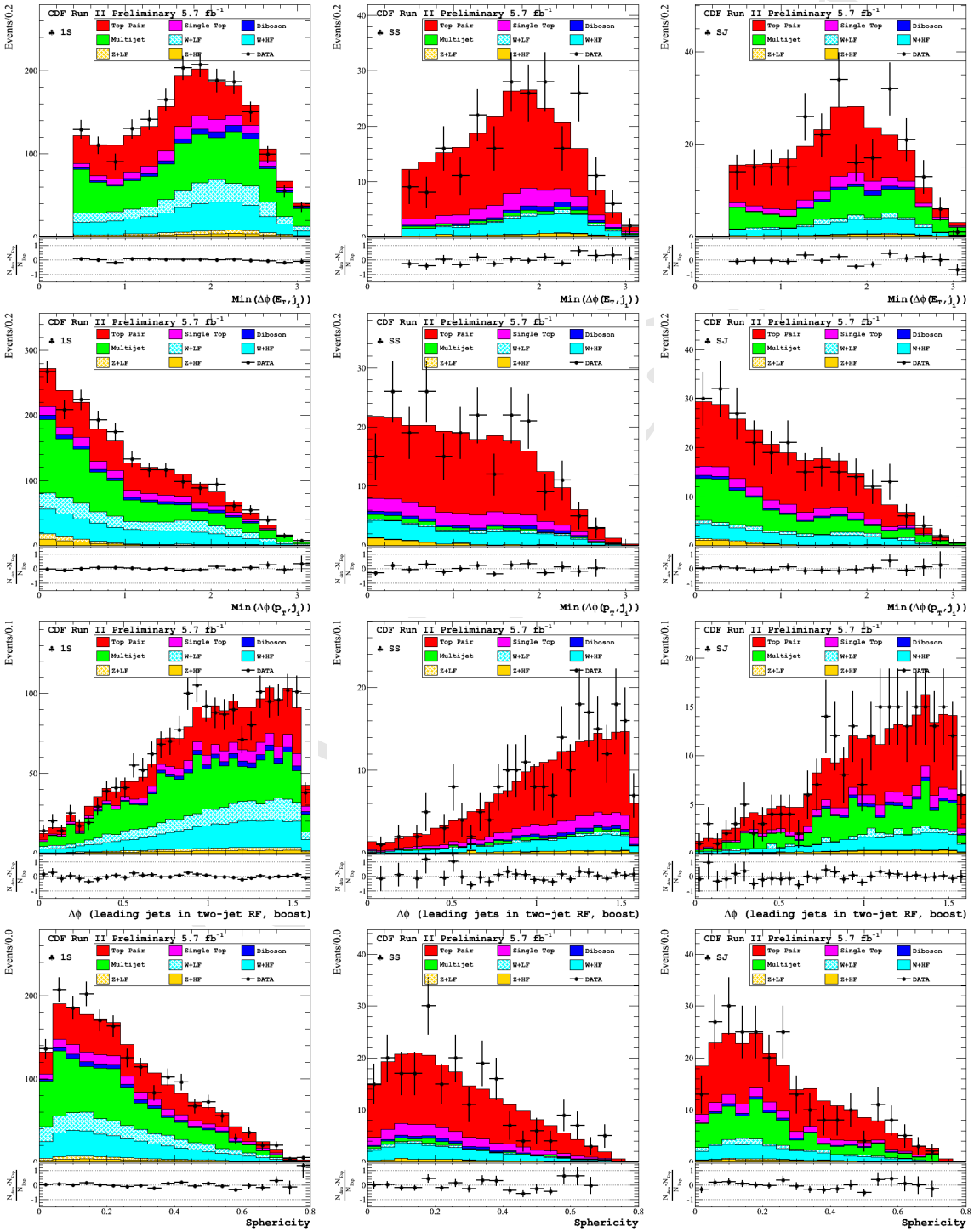
CDF Run II Preliminary 5.7 fb^{-1}
♣ 1S
♣ SS
♣ SJ
Top Pair
Single Top
Diboson
Multijet
W+LF
W+HF
Z+LF
Z+HF
DATA
Events/0.2
Events/0.1
Events/0.0
Min($\Delta\phi(\not{E}_T, j_1)$)
Min($\Delta\phi(\not{p}_T, j_1)$)
$\Delta\phi$ (leading jets in two-jet RF, boost)
Sphericity
$N_{data}-N_{bg}$ / N_{bg}

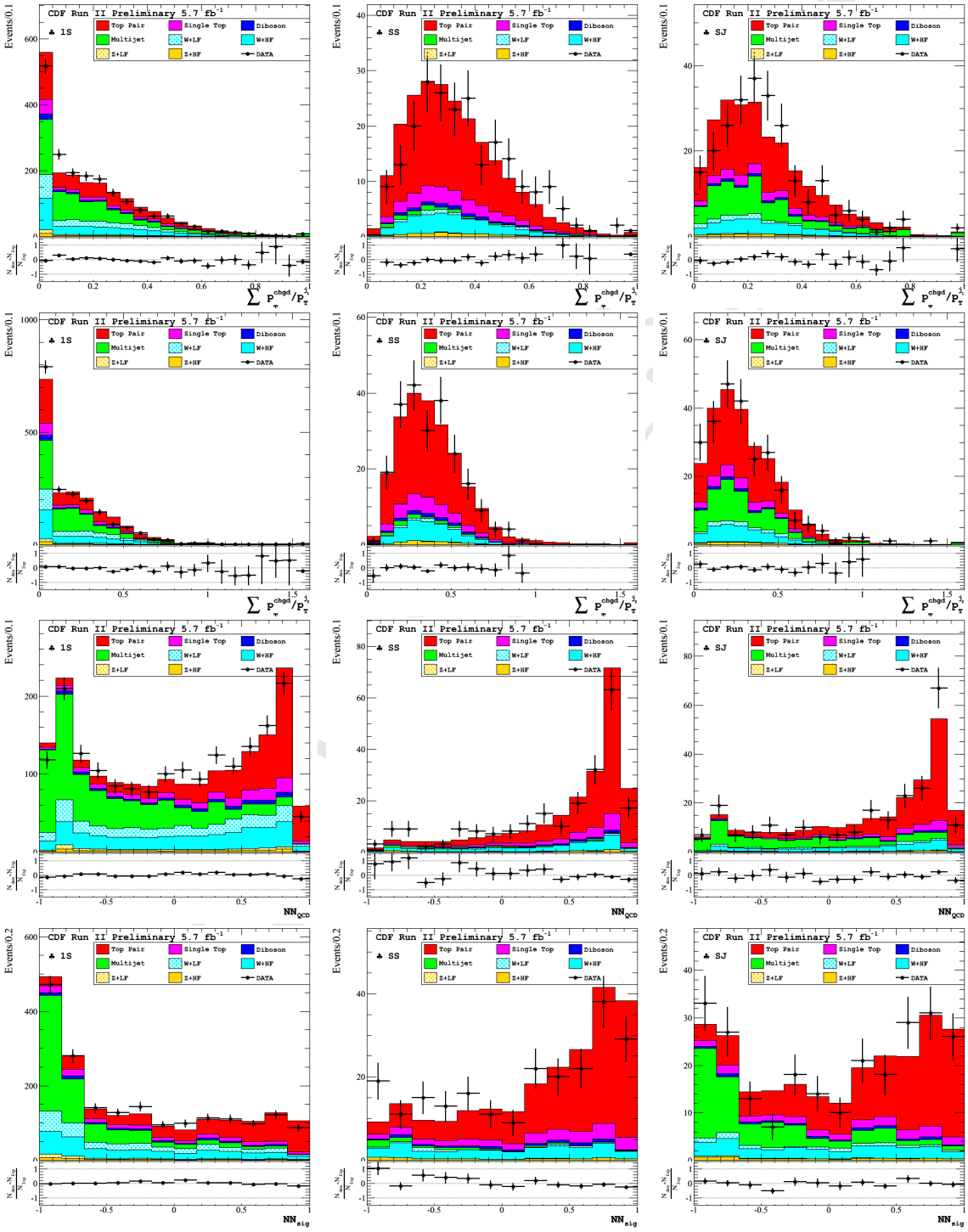
CDF Run II Preliminary 5.7 fb^{-1}
1S
SS
SJ
Top Pair
Single Top
Diboson
Multijet
W+LF
W+HF
Z+LF
Z+HF
DATA
Events/0.1
Events/0.2
$\sum p_T^{chgd}/p_T^{\tau_1}$
NN_{QCD}
NN_{sig}
$N_{data}-N_{bg}$ / N_{tot}

C.4 PreSelection

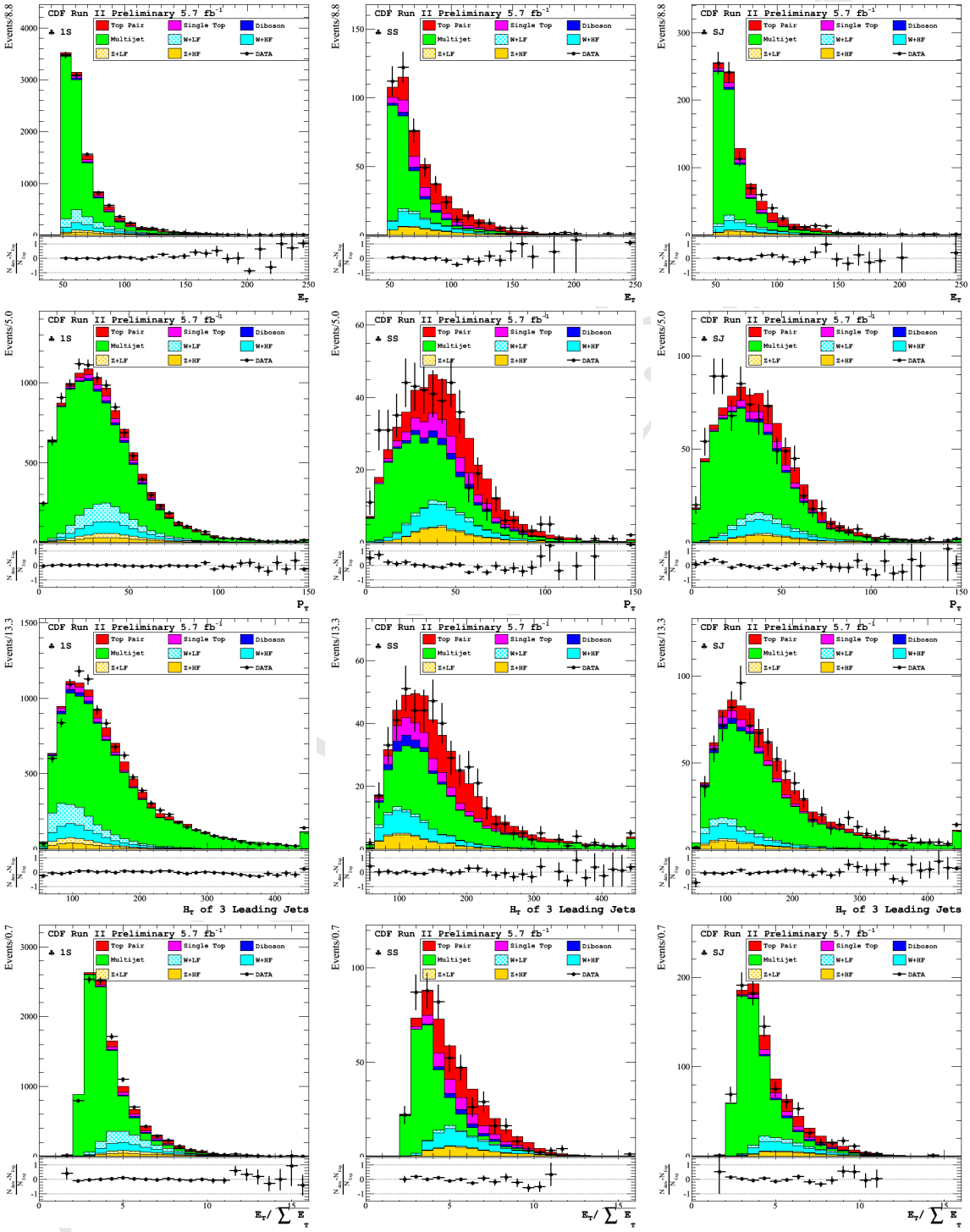

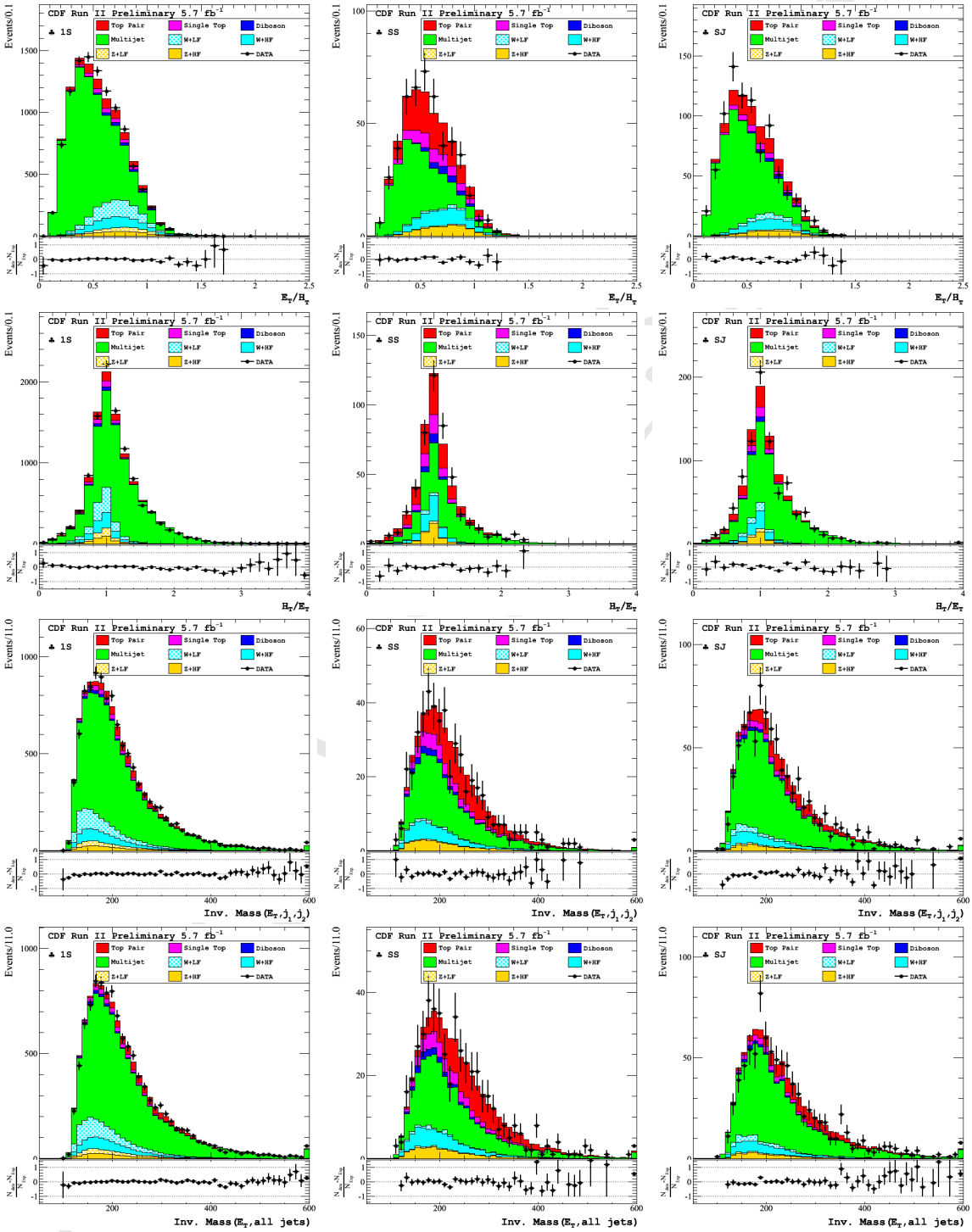
CDF Run II Preliminary 5.7 fb^{-1}
1S
SS
SJ
Top Pair
Single Top
Diboson
Multijet
W+LF
W+HF
Z+LF
Z+HF
DATA
Events/0.1
Events/11.0
E_T/H_T
H_T/E_T
Inv. Mass(E_T,j_1,j_2)
Inv. Mass(E_T,all jets)
$N_{data}-N_{bg}$ / N_{bg}

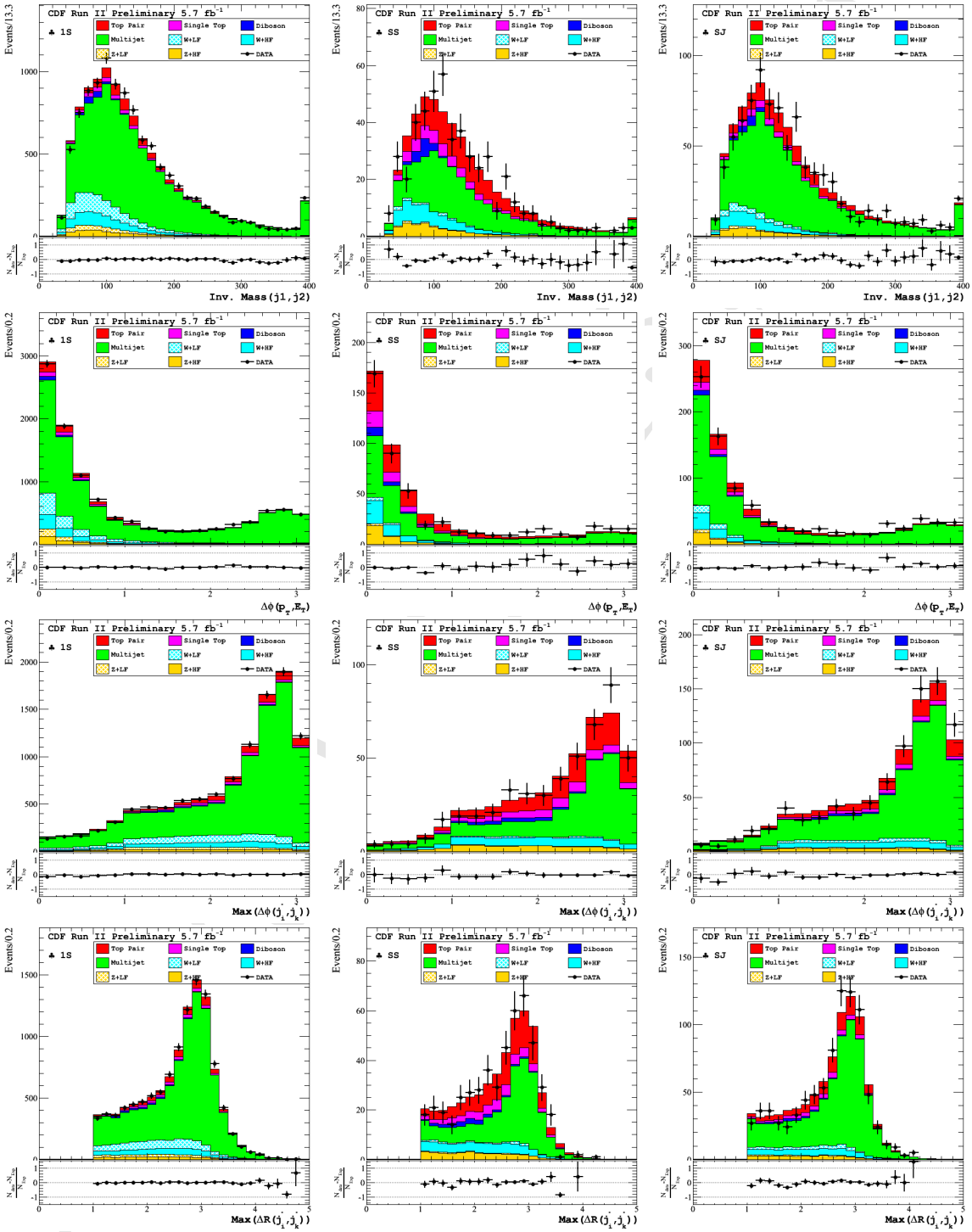
CDF Run II Preliminary 5.7 fb^{-1}
1S
SS
SJ
Top Pair
Single Top
Diboson
Multijet
W+LF
W+HF
Z+LF
Z+HF
DATA
Events/13.3
Inv. Mass(j1,j2)
Events/0.2
$\Delta\phi(\not{p}_T,\not{E}_T)$
Max($\Delta\phi(j_i,j_k)$)
Max($\Delta R(j_i,j_k)$)
$N_{data}-N_{bg}$ / N_{tot}

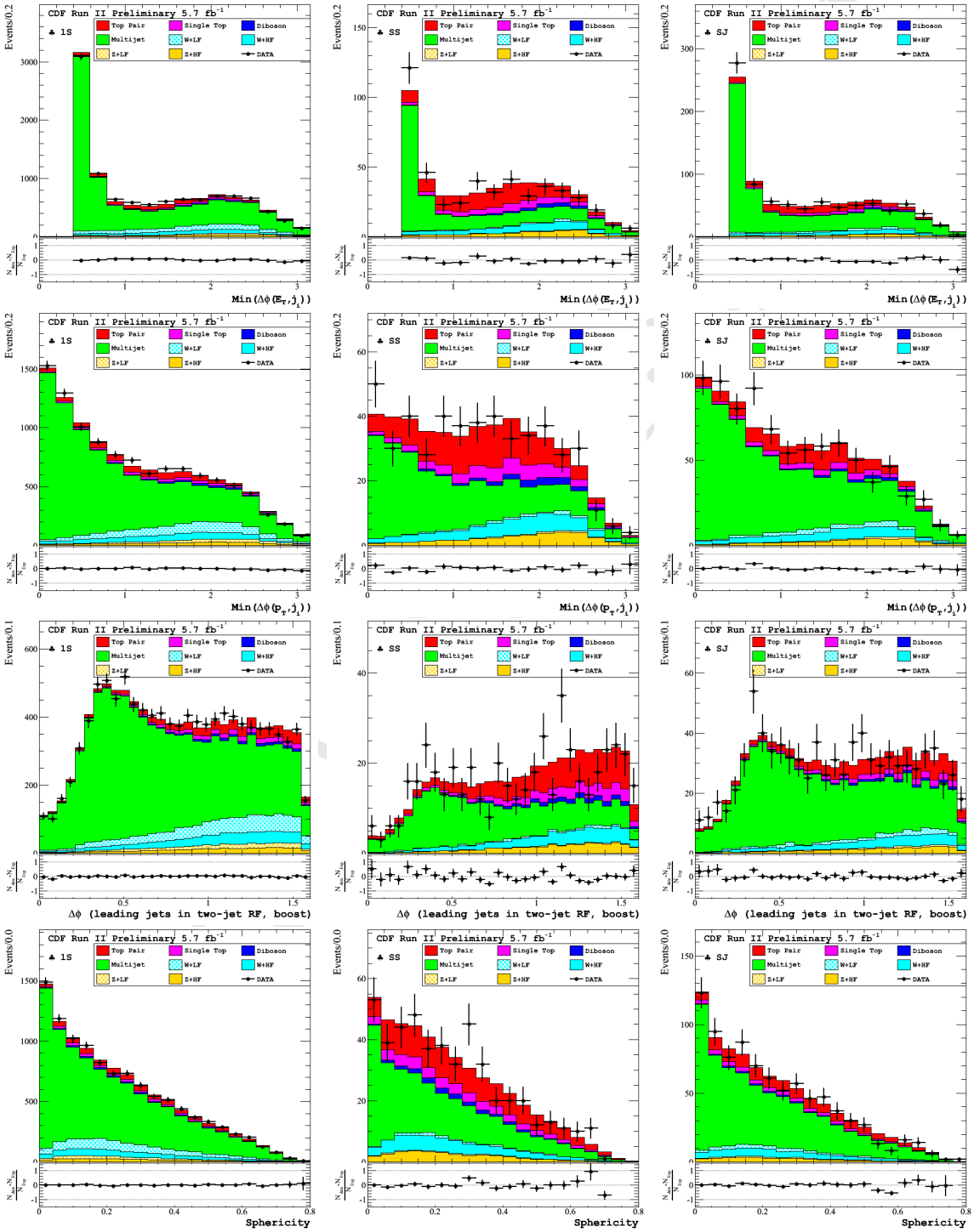
CDF Run II Preliminary 5.7 fb^{-1}
1S
SS
SJ
Top Pair
Single Top
Diboson
Multijet
W+LF
W+HF
Z+LF
Z+HF
DATA
Events/0.2
Events/0.1
Events/0.0
Min($\Delta\phi(\not{E}_T, j_1)$)
Min($\Delta\phi(\not{p}_T, j_1)$)
$\Delta\phi$ (leading jets in two-jet RF, boost)
Sphericity
$N_{data}-N_{bg}$ / N_{bg}

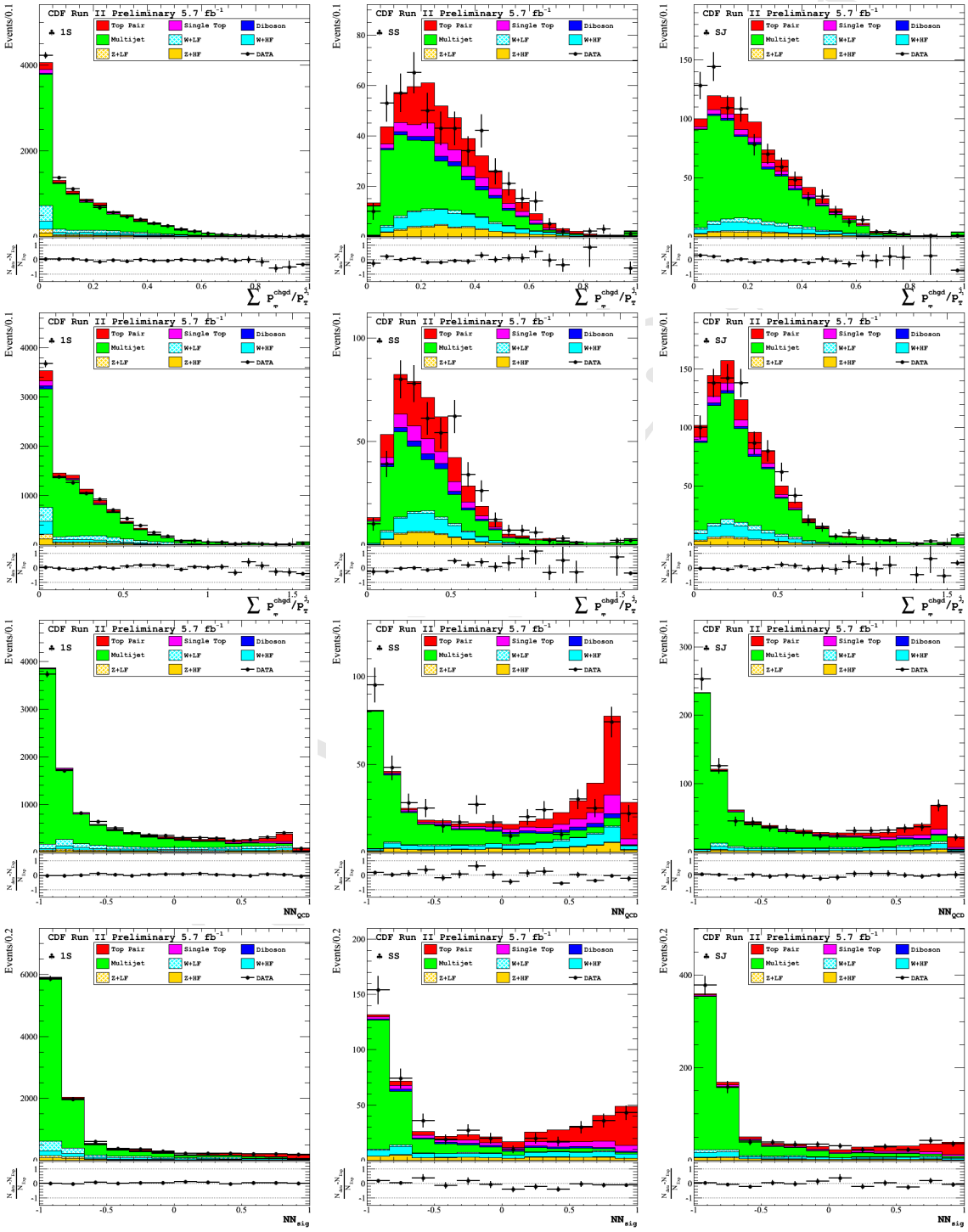
CDF Run II Preliminary 5.7 fb^{-1}
1S
SS
SJ
Top Pair
Single Top
Diboson
Multijet
W+LF
W+HF
Z+LF
Z+HF
DATA
Events/0.1
Events/0.2
$\sum p_T^{chgd}/p_T^{j_1}$
NN_{QCD}
NN_{sig}
$\frac{N_{data}-N_{bg}}{N_{bg}}$

C.5 Lower_ttbar

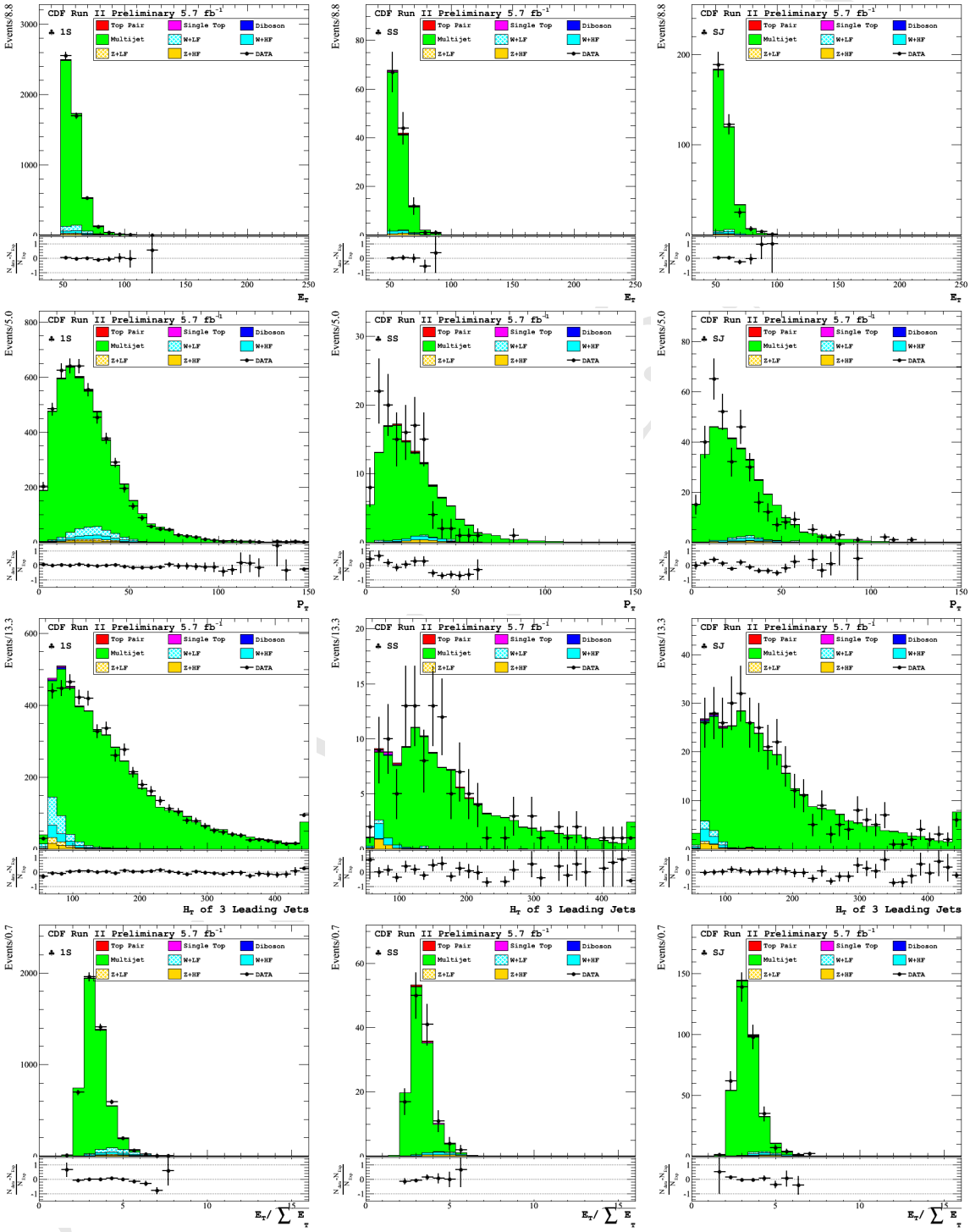

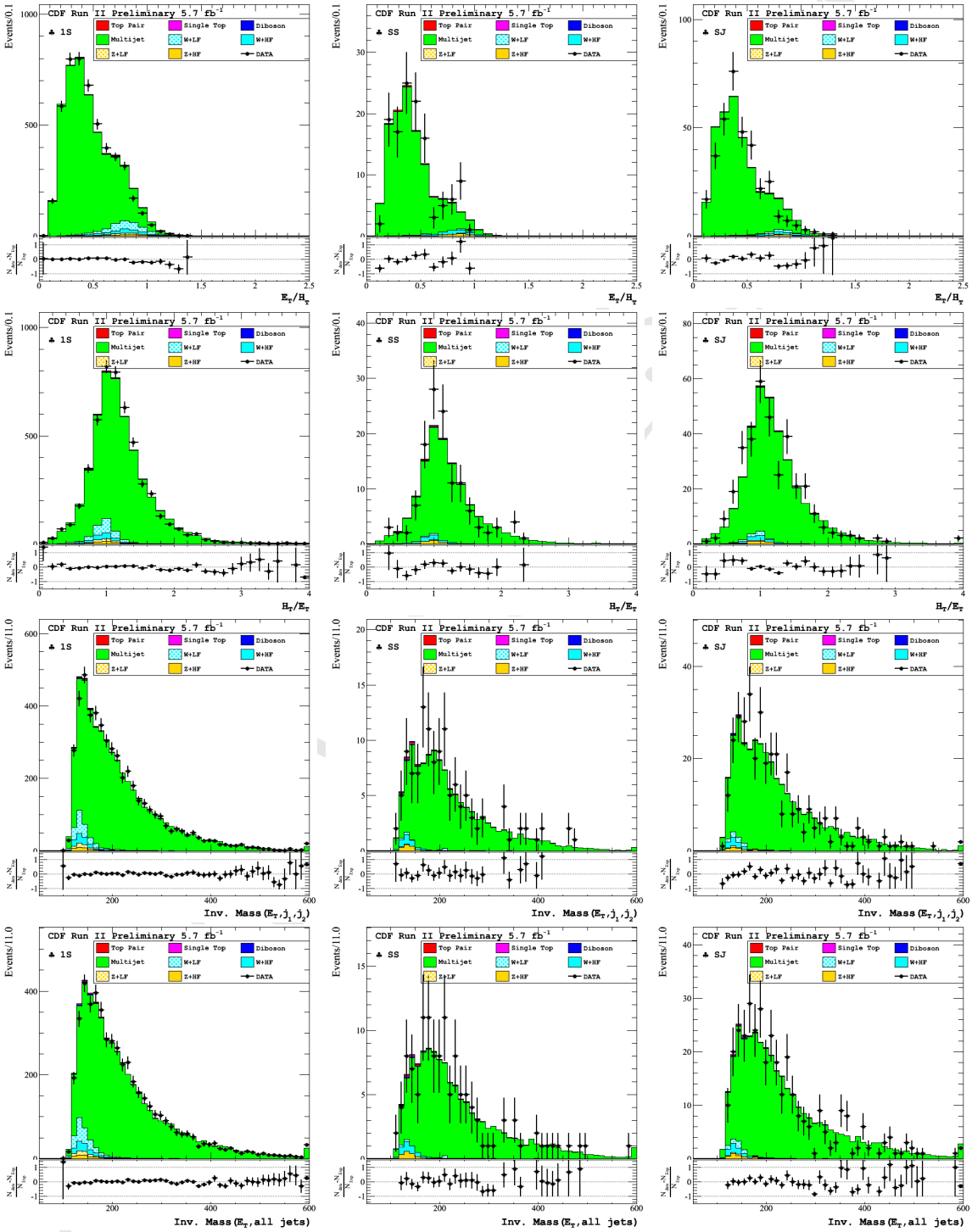
CDF Run II Preliminary 5.7 fb^{-1}
1S
SS
SJ
Top Pair
Single Top
Diboson
Multijet
W+LF
W+HF
Z+LF
Z+HF
DATA
Events/0.1
Events/11.0
E_T/H_T
H_T/E_T
Inv. Mass(E_T,j_1,j_2)
Inv. Mass(E_T,all jets)
$N_{data}-N_{bg}$ / N_{bg}

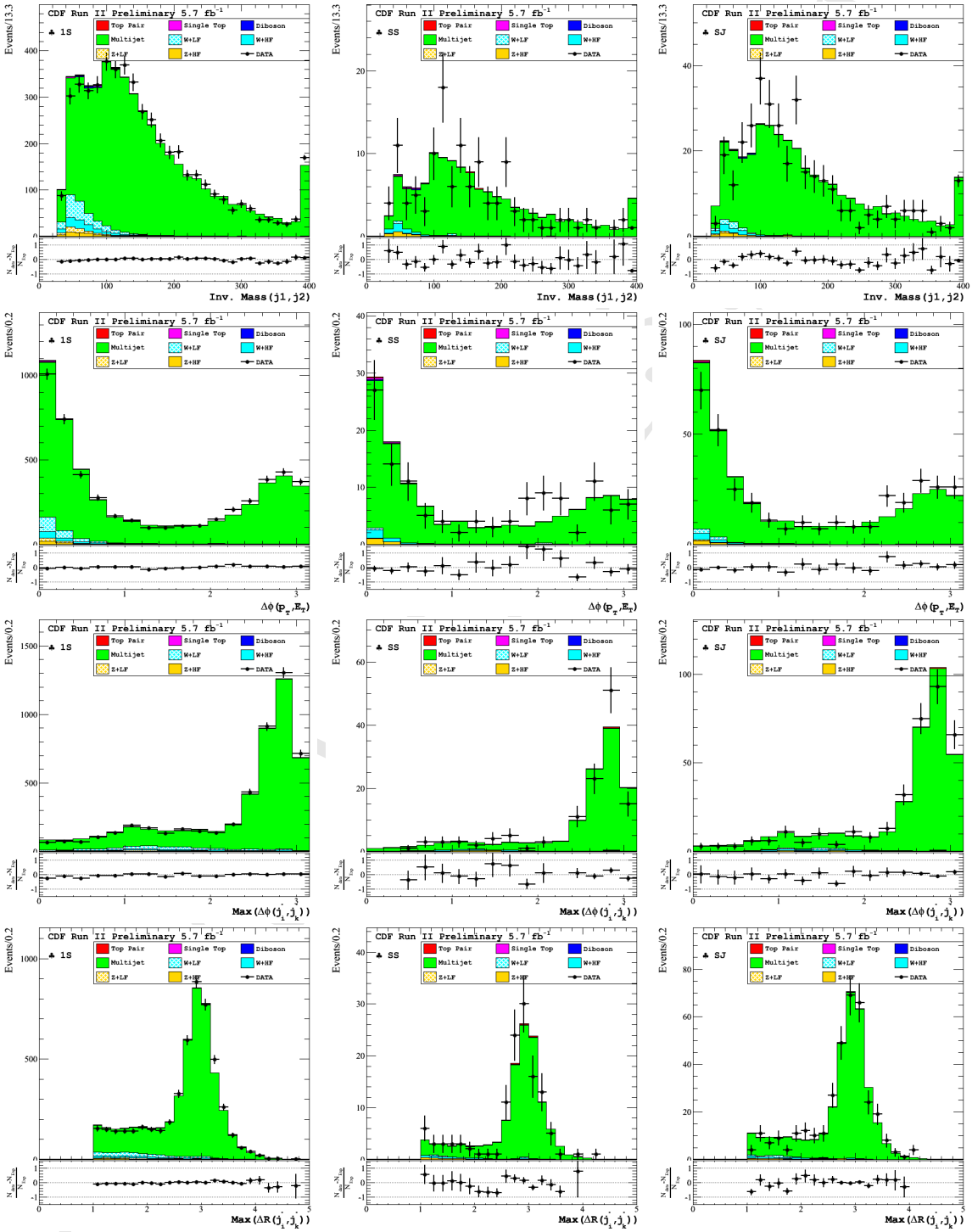
CDF Run II Preliminary 5.7 fb^{-1}
1S
SS
SJ
Top Pair
Single Top
Diboson
Multijet
W+LF
W+HF
Z+LF
Z+HF
DATA
Events/13.3
Inv. Mass(j1,j2)
Events/0.2
$\Delta\phi(p_T, E_T)$
Max($\Delta\phi(j_i, j_k)$)
Max($\Delta R(j_i, j_k)$)
$N_{data}-N_{bg}$ / N_{bg}

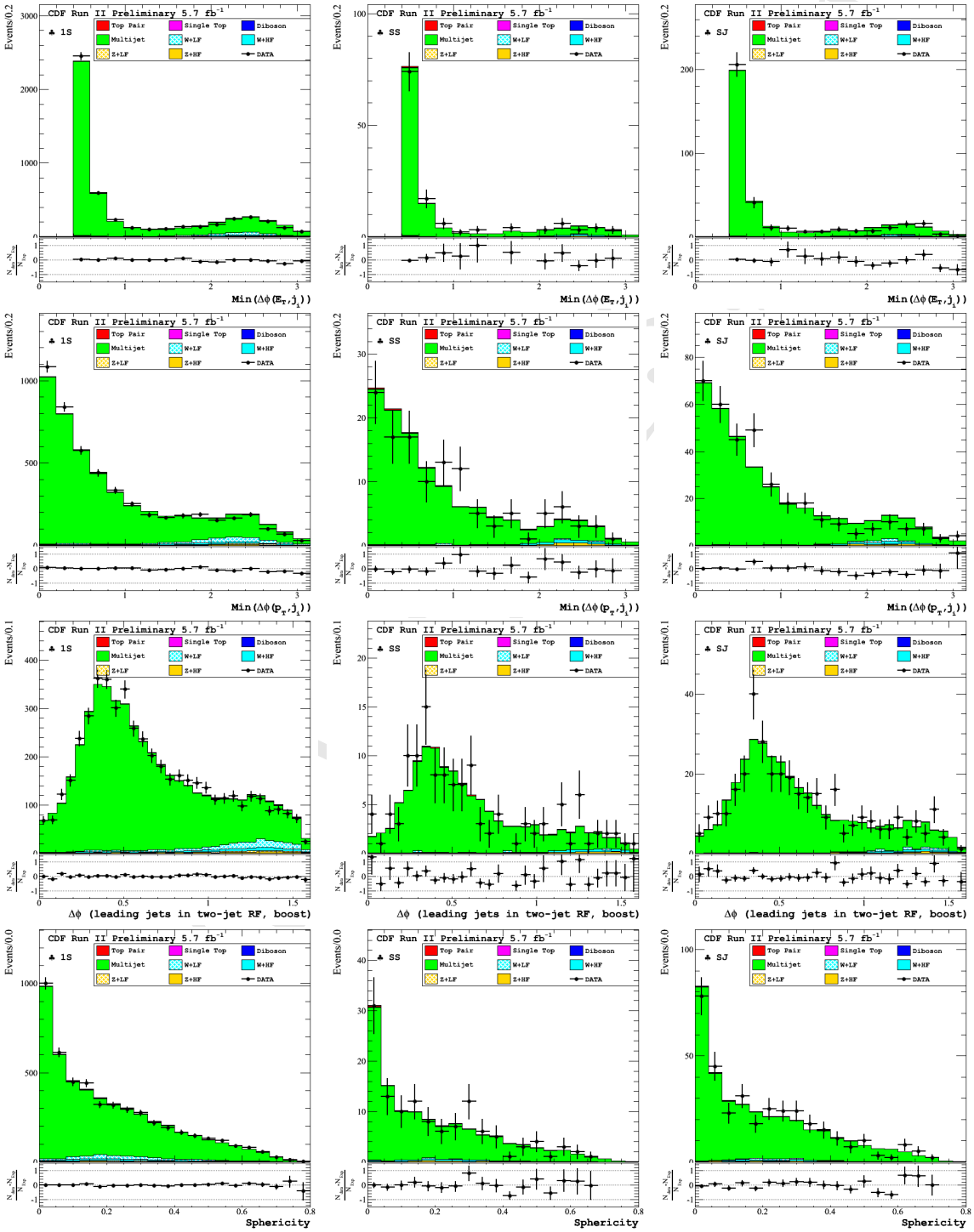
CDF Run II Preliminary 5.7 fb^{-1}
1S
SS
SJ
Top Pair
Single Top
Diboson
Multijet
W+LF
W+HF
Z+LF
Z+HF
DATA
Events/0.2
Events/0.1
Events/0.0
Min($\Delta\phi(\not{E}_T, j_1)$)
Min($\Delta\phi(\not{p}_T, j_1)$)
$\Delta\phi$ (leading jets in two-jet RF, boost)
Sphericity
$N_{data}-N_{bg}$ / N_{bg}

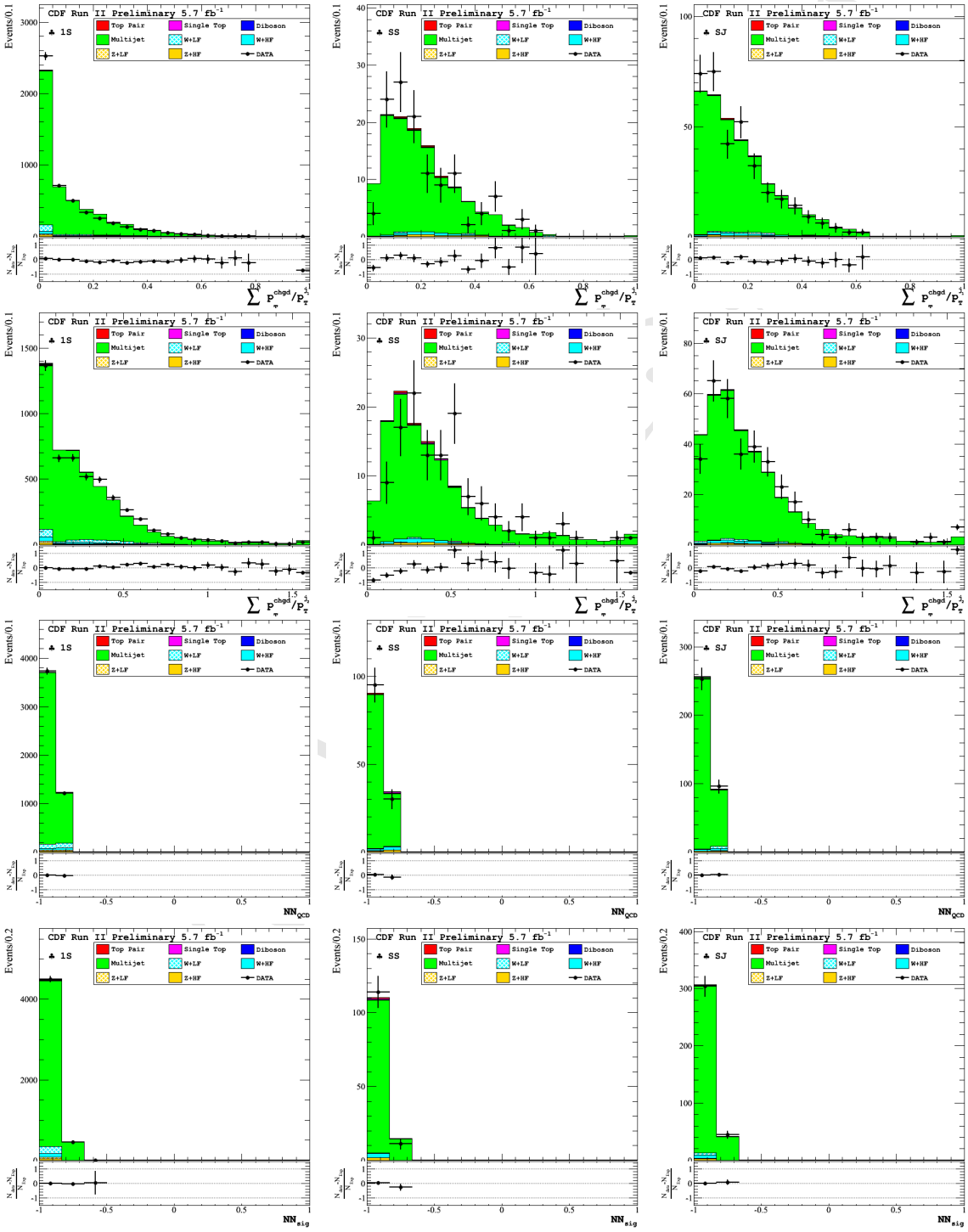
CDF Run II Preliminary 5.7 fb^{-1}
1S
SS
SJ
Top Pair
Single Top
Diboson
Multijet
W+LF
W+HF
Z+LF
Z+HF
DATA
Events/0.1
Events/0.2
$\sum p_T^{chgd}/p_T^{j_1}$
NN_{QCD}
NN_{sig}
$\frac{N_{data}-N_{bg}}{N_{bg}}$

C.6 Inter_ttbar

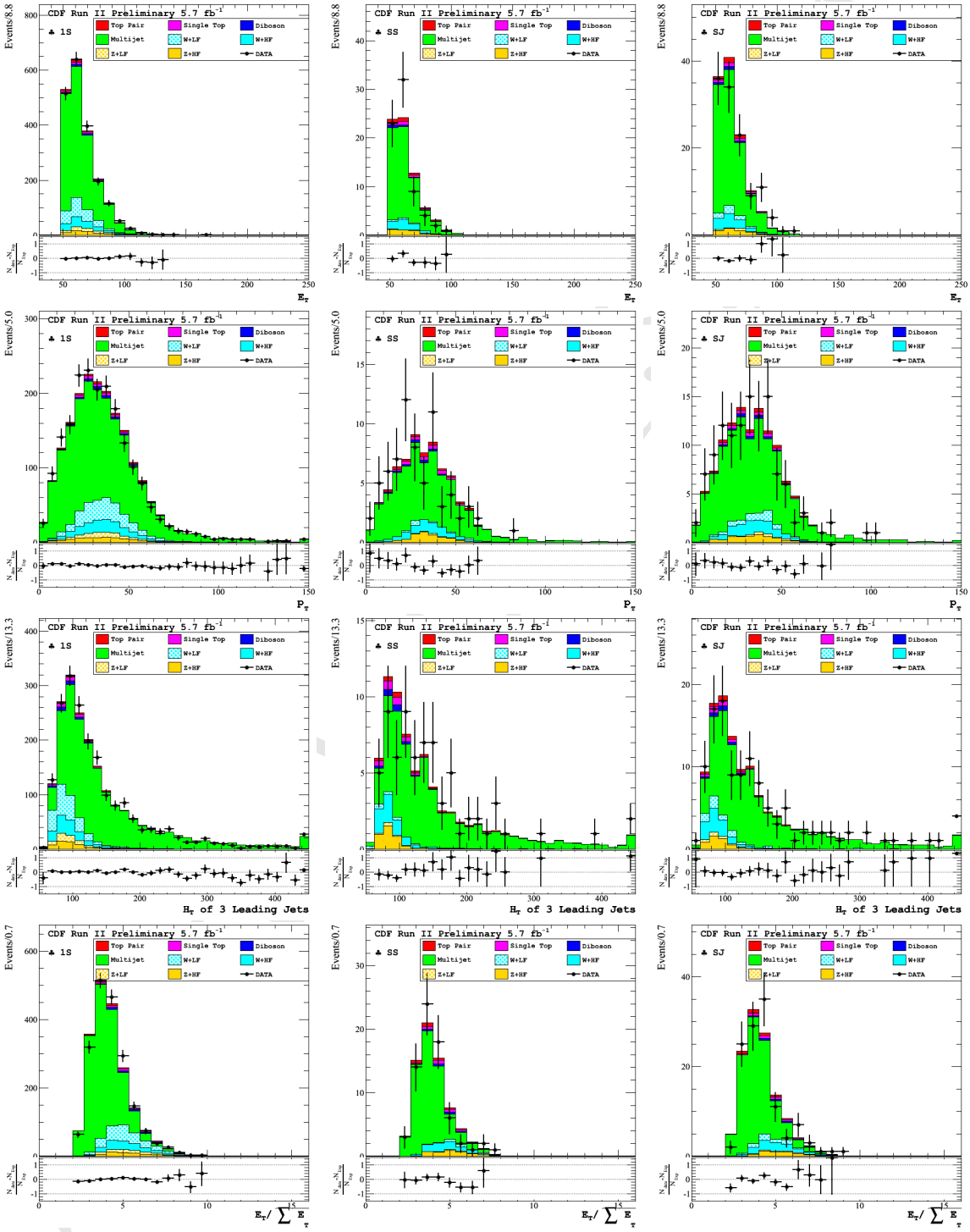

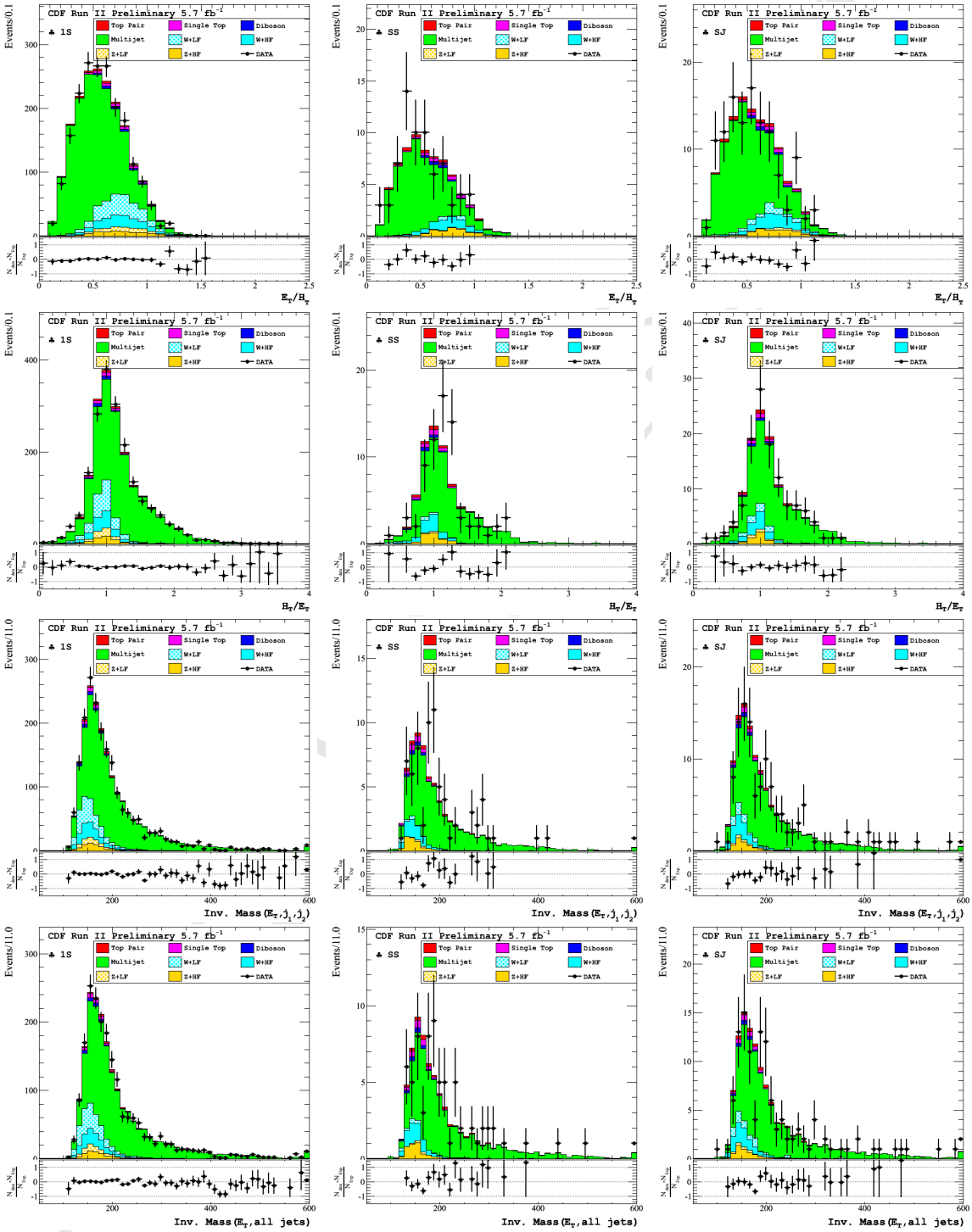
CDF Run II Preliminary 5.7 fb^{-1}
1S
SS
SJ
Top Pair
Single Top
Diboson
Multijet
W+LF
W+HF
Z+LF
Z+HF
DATA
Events/0.1
Events/11.0
E_T/H_T
H_T/E_T
Inv. Mass(E_T,j_1,j_2)
Inv. Mass(E_T,all jets)
$N_{Data}-N_{bg}$ / N_{bg}

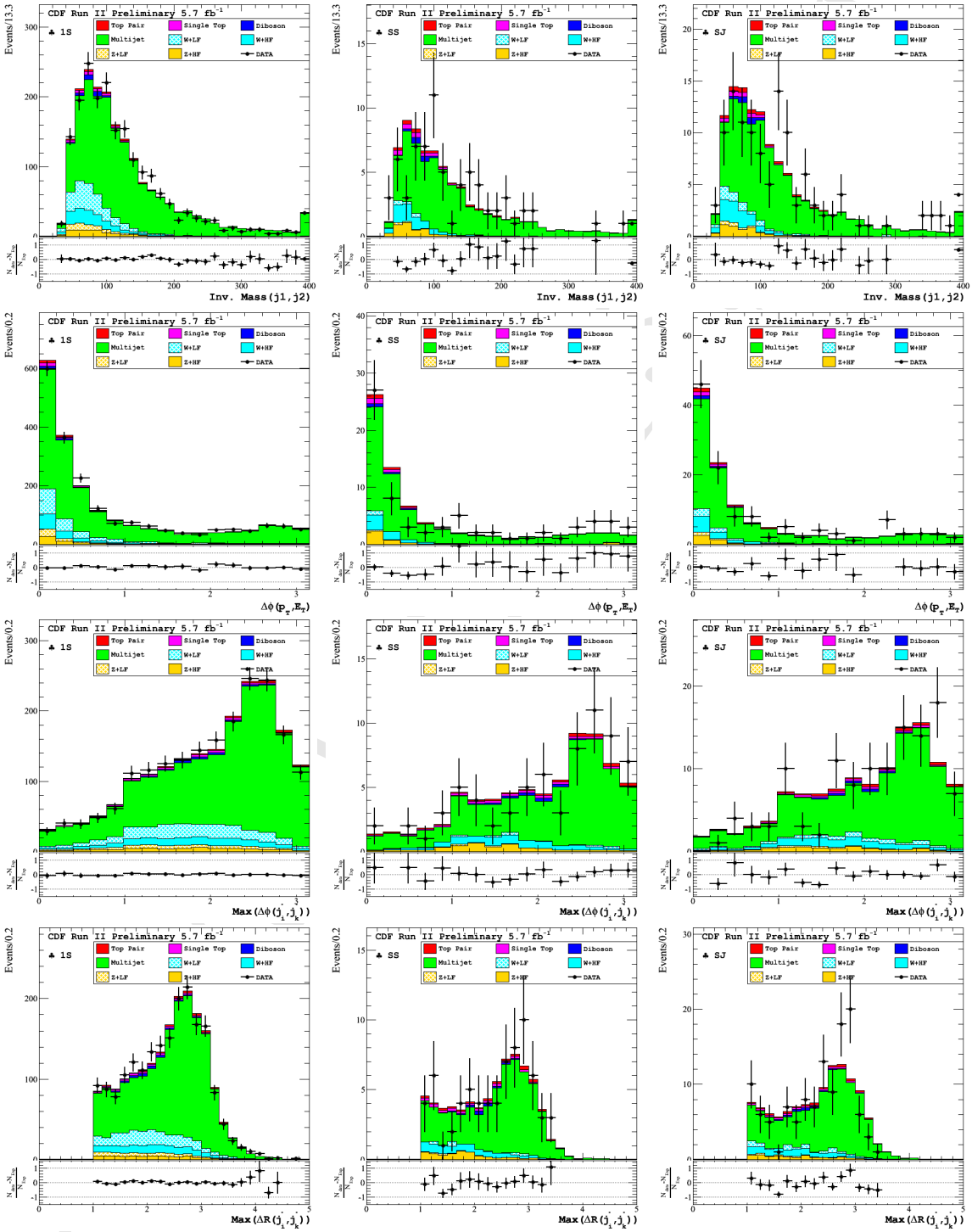
CDF Run II Preliminary 5.7 fb^{-1}
1S
SS
SJ
Top Pair
Single Top
Diboson
Multijet
W+LF
W+HF
Z+LF
Z+HF
DATA
Events/13.3
Events/0.2
Inv. Mass(j1,j2)
$\Delta\phi(\not{p}_T,\not{E}_T)$
Max($\Delta\phi(j_i,j_k)$)
Max($\Delta R(j_i,j_k)$)
$N_{data}-N_{bg}$ / N_{bg}

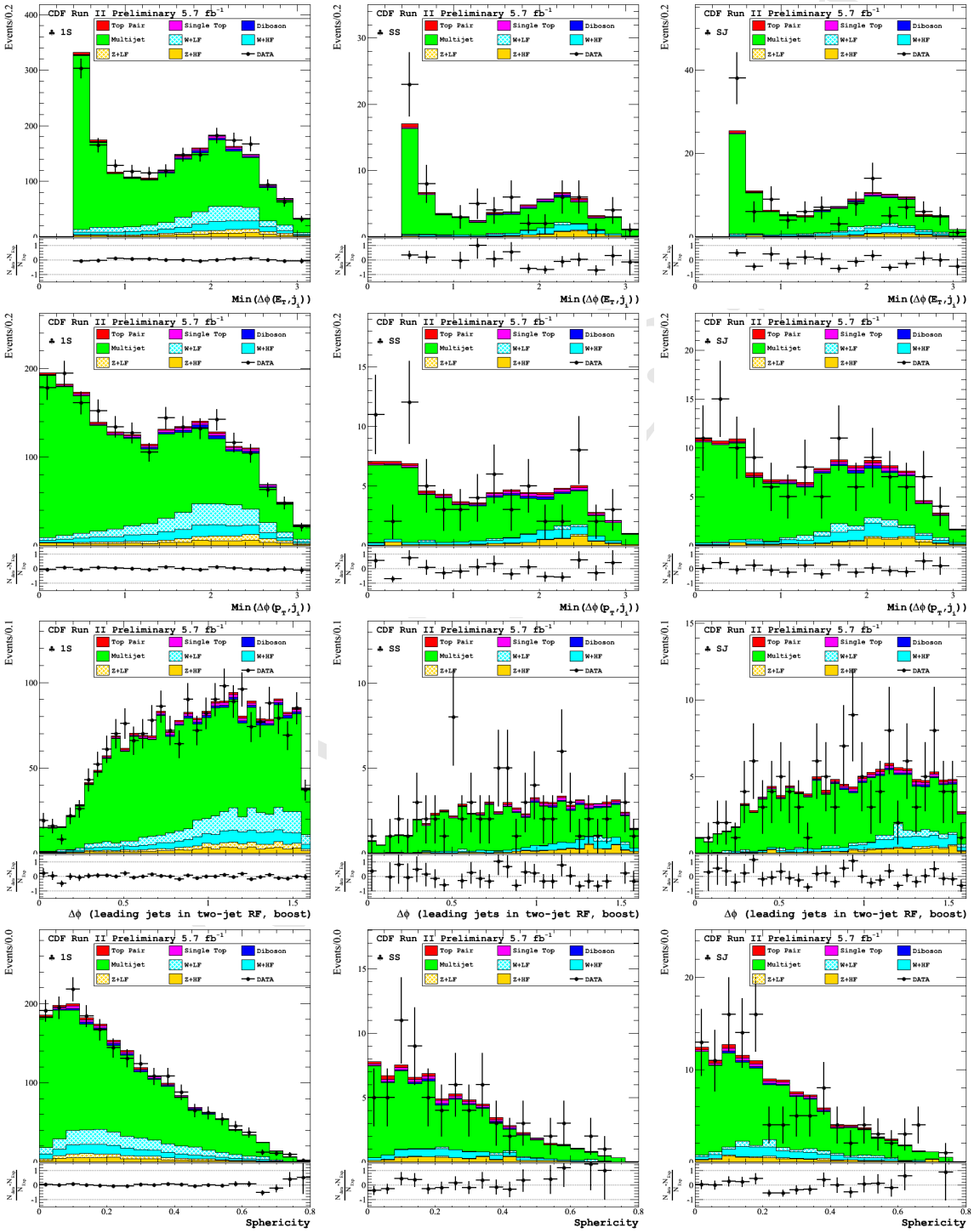
CDF Run II Preliminary 5.7 fb^{-1}
1S
SS
SJ
Top Pair
Single Top
Diboson
Multijet
W+LF
W+HF
Z+LF
Z+HF
DATA
Events/0.2
Events/0.1
Events/0.0
Min($\Delta\phi(\not{E}_T, j_1)$)
Min($\Delta\phi(\not{p}_T, j_1)$)
$\Delta\phi$ (leading jets in two-jet RF, boost)
Sphericity
$N_{data}-N_{bg}$ / N_{bg}

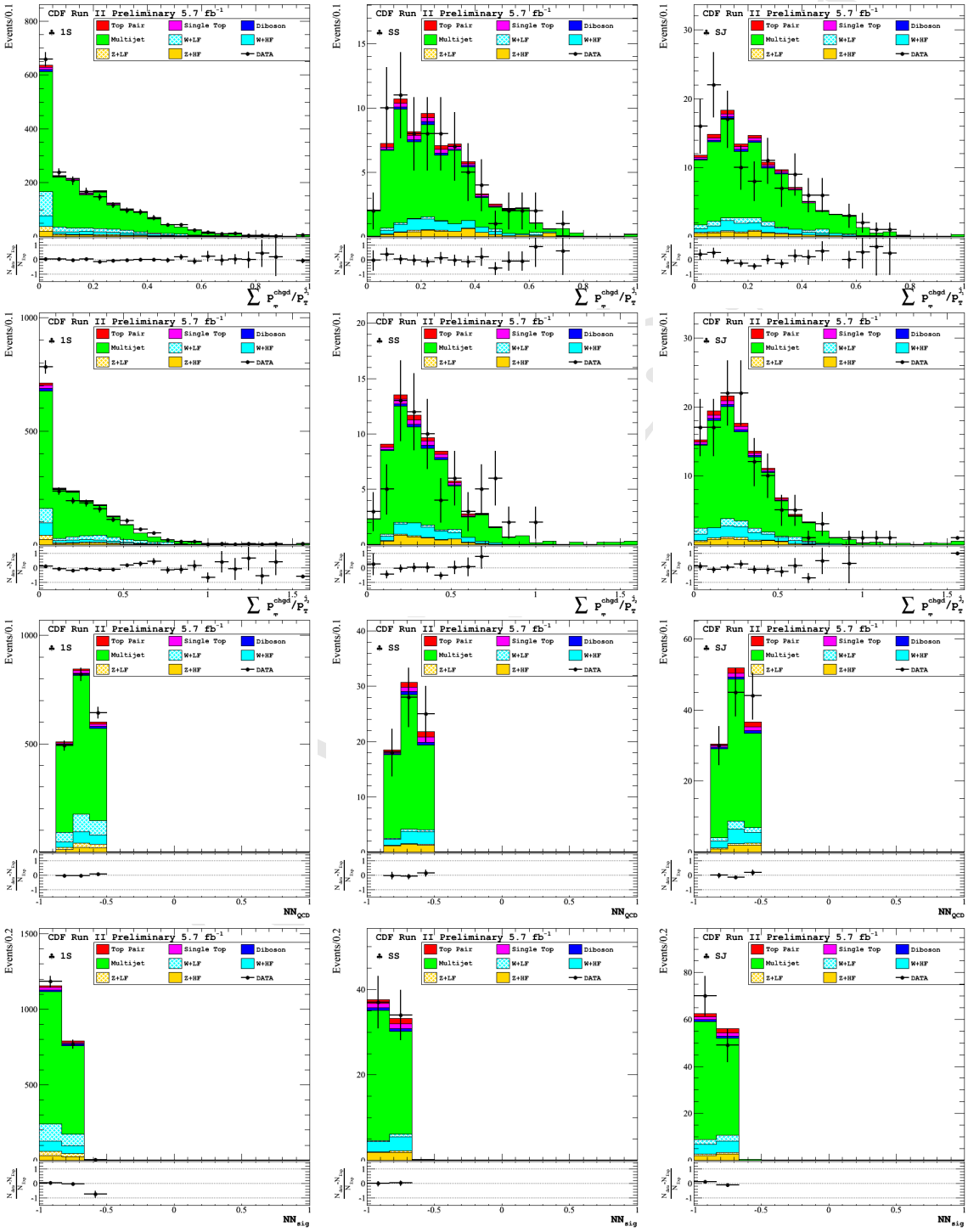
CDF Run II Preliminary 5.7 fb^{-1}
1S
SS
SJ
Top Pair
Single Top
Diboson
Multijet
W+LF
W+HF
Z+LF
Z+HF
DATA
Events/0.1
Events/0.2
$\sum p_T^{chgd}/p_T^{j_1}$
NN_{QCD}
NN_{sig}
$N_{data}-N_{bg}$ / N_{bg}

C.7 SigReg_ttbar

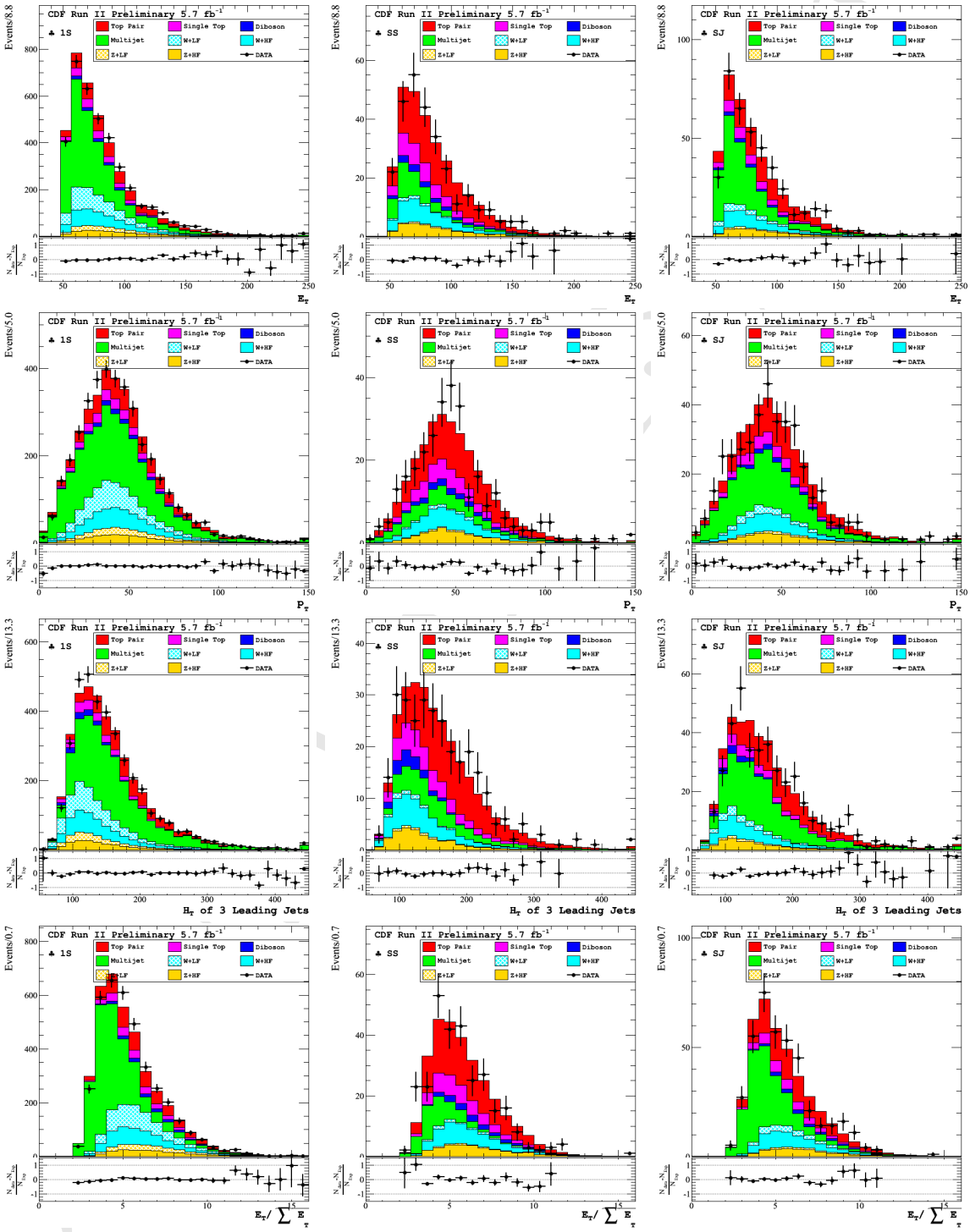

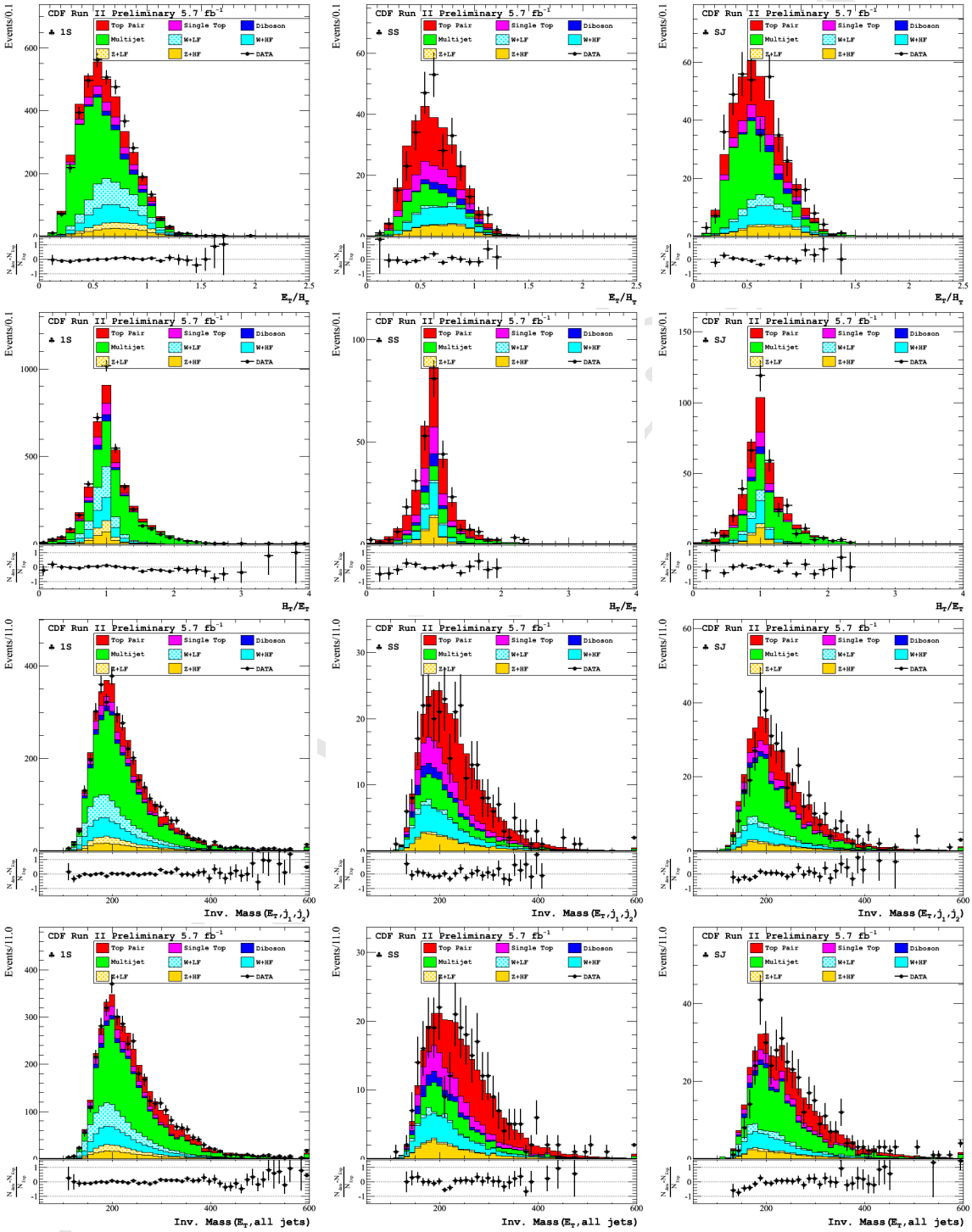
CDF Run II Preliminary 5.7 fb^{-1}
♣ 1S
♣ SS
♣ SJ
Top Pair
Single Top
Diboson
Multijet
W+LF
W+HF
Z+LF
Z+HF
DATA
Events/0.1
Events/11.0
E_T/H_T
H_T/E_T
Inv. Mass(E_T,j_1,j_2)
Inv. Mass(E_T,all jets)
$N_{data}-N_{bg}$ / N_{bg}

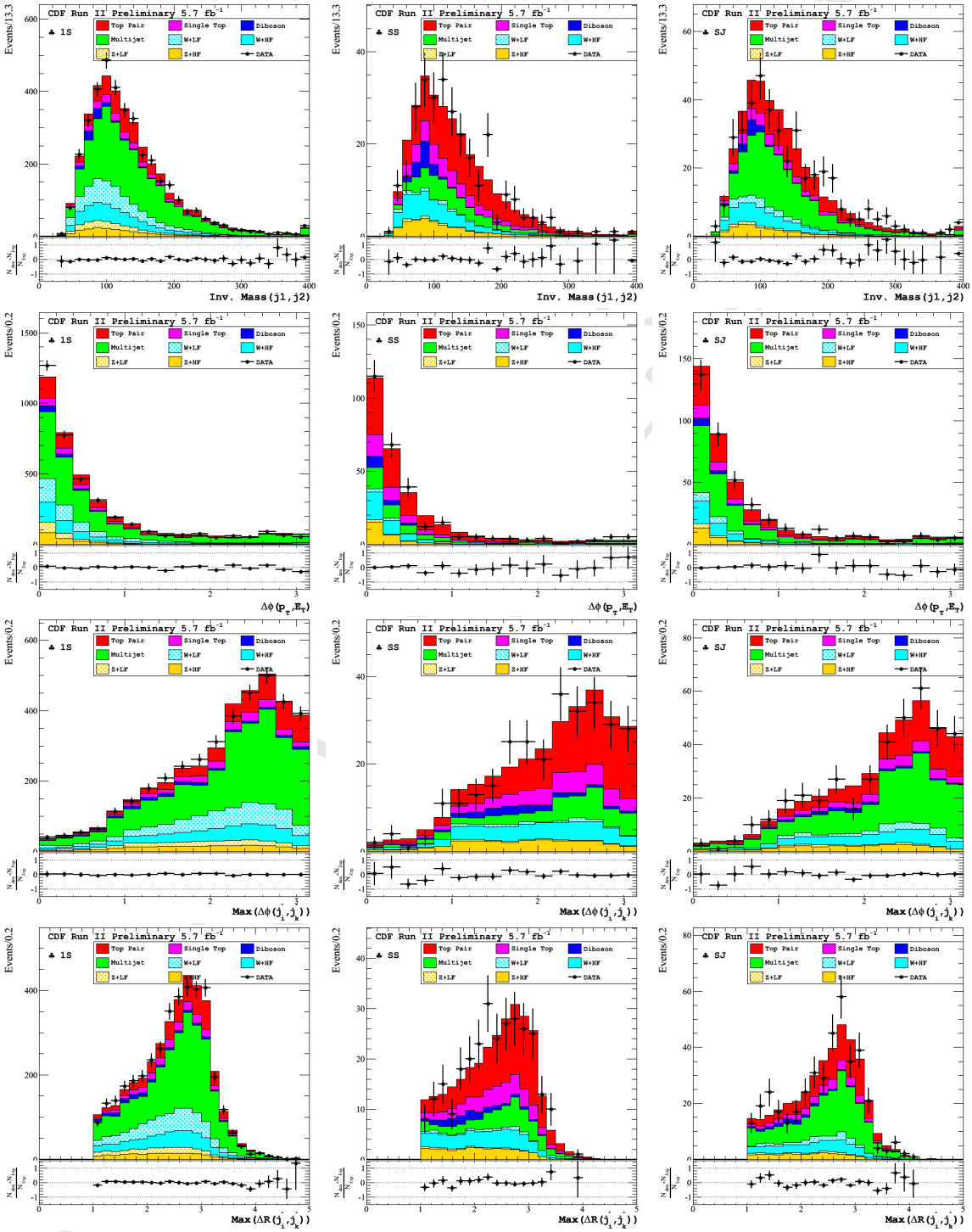
CDF Run II Preliminary 5.7 fb^{-1}
1S
SS
SJ
Top Pair
Single Top
Diboson
Multijet
W+LF
W+HF
Z+LF
Z+HF
DATA
Events/13.3
Events/0.2
Inv. Mass(j1,j2)
$\Delta\phi(p_T, E_T)$
Max($\Delta\phi(j_i, j_k)$)
Max($\Delta R(j_i, j_k)$)
$N_{data}-N_{bg}$ / N_{bg}

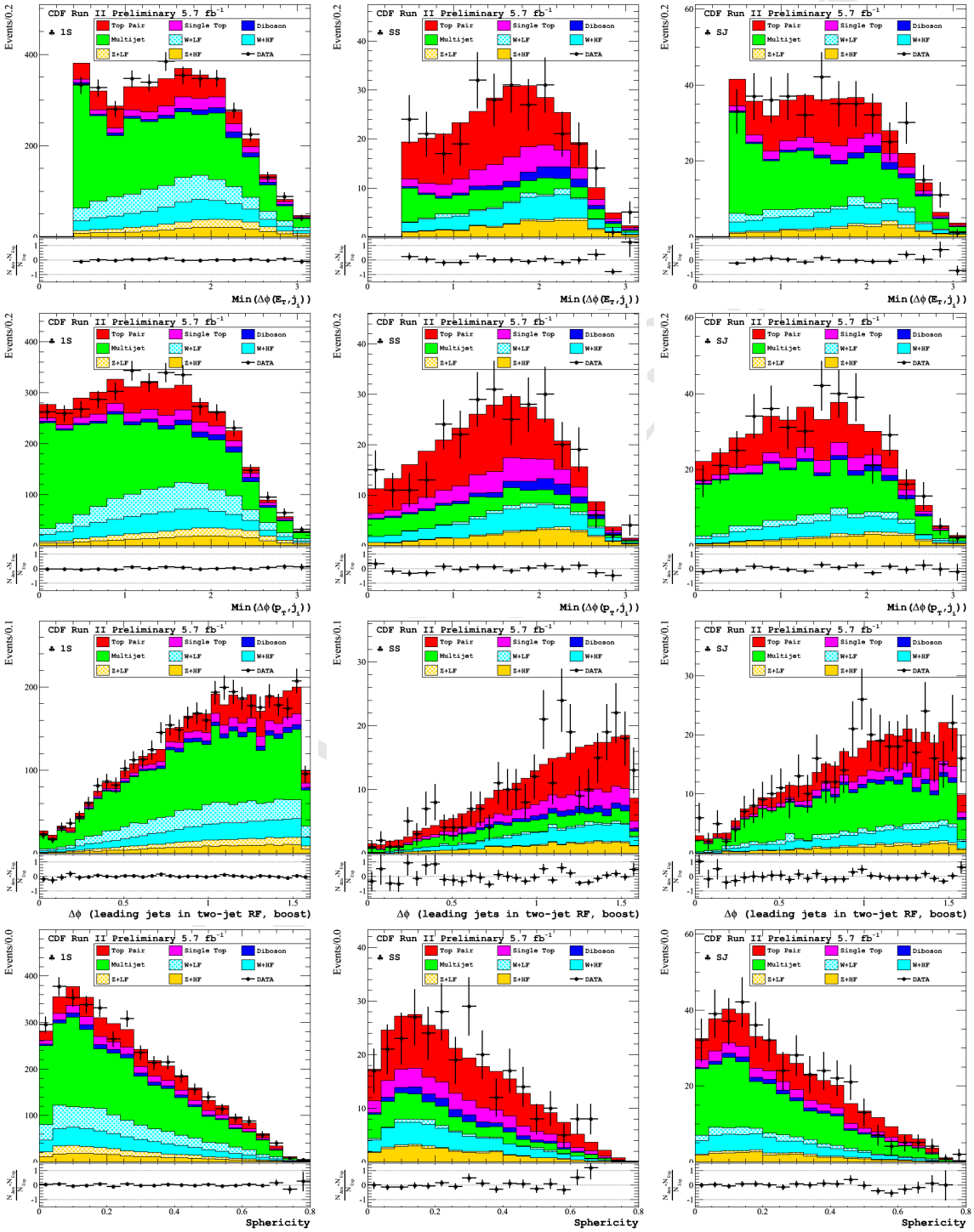
CDF Run II Preliminary 5.7 fb^{-1}
1S
SS
SJ
Top Pair
Single Top
Diboson
Multijet
W+LF
W+HF
Z+LF
Z+HF
DATA
Events/0.2
Events/0.1
Events/0.0
Min($\Delta\phi(\not{E}_T, j_1)$)
Min($\Delta\phi(\not{p}_T, j_1)$)
$\Delta\phi$ (leading jets in two-jet RF, boost)
Sphericity
$N_{data}-N_{bg}$ / N_{bg}

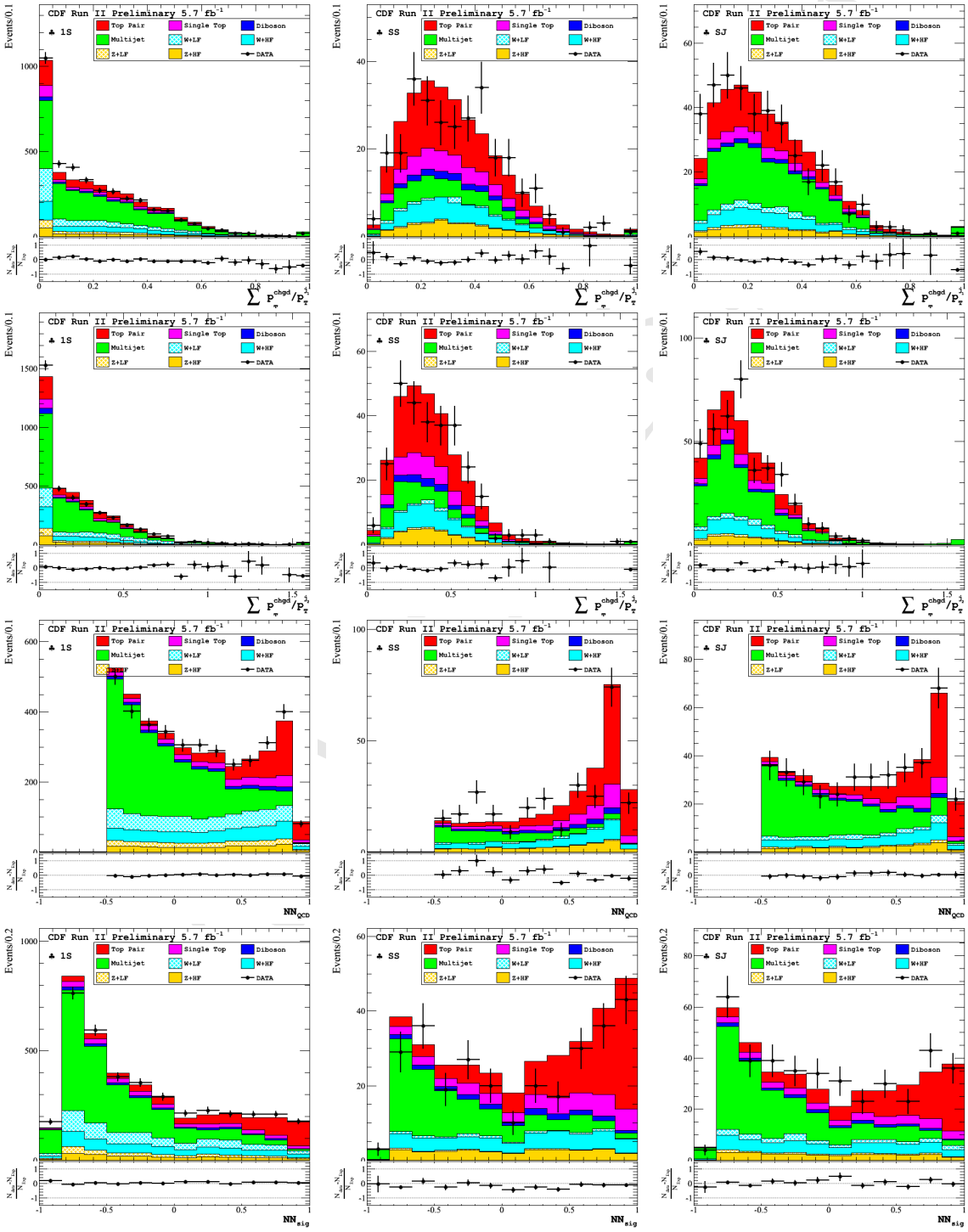
CDF Run II Preliminary 5.7 fb^{-1}
1S
SS
SJ
Top Pair
Single Top
Diboson
Multijet
W+LF
W+HF
Z+LF
Z+HF
DATA
Events/0.1
Events/0.2
$\sum p_T^{chgd}/p_T^{\tau_1}$
NN_{QCD}
NN_{sig}
$N_{data}-N_{bg}$ / N_{bg}